A PRELIMINARY STUDY OF THE EFFECTS OF A FRONT WHEEL STEERING STABILIZER AND OF FIFTH WHEEL ANTI-JACKKNIFING DEVICES ON ARTICULATED VEHICLE RESPONSE CHARACTERISTICS

By

CLINE TURNER YOUNG II

Bachelor of Science

United States Merchant Marine Academy

Kings Point, New York

1973

Submitted to the Faculty of the Graduate College
of the Oklahoma State University
in partial fulfillment of the requirements
for the Degree of
MASTER OF SCIENCE
May, 1976

A PRELIMINARY STUDY OF THE EFFECTS OF A FRONT WHEEL STEERING STABILIZER AND OF FIFTH WHEEL ANTI-JACKKNIFING DEVICES ON ARTICULATED VEHICLE RESPONSE CHARACTERISTICS

Thesis Approved:

Donald E. Boyd
Thesis Adviser

Larry D. Zirbel

R L Lowery

N N Durham
Dean of the Graduate College

PREFACE

The purpose of this thesis was to determine whether or not a fifth wheel anti-jackknifing device would have a positive effect in allowing an articulated vehicle to be brought under control in the early stages of jackknifing. A computer program was developed to solve the equations of motion.

I would like to express my appreciation to my major adviser, Dr. Donald E. Boyd, for his guidance and assistance, and particularly for his inexhaustible supply of patience and good humor during the trying times encountered within this study. Appreciation is also expressed to the other committee members, Dr. Richard L. Lowry and Dr. Larry D. Zirkle, for their assistance in the preparation of the final manuscript.

I would also like to acknowledge the invaluable assistance provided by Mr. David Turney in all phases of this study. A note of thanks is given to Mr. Steve Grundmann and Mr. Ervind Amin for their helpful suggestions. In addition, appreciation is extended to my cousin, Mr. James Pletcher, for his understanding and encouragement.

Finally, gratitude is expressed to the School of Mechanical and Aerospace Engineering for providing a teaching assistantship which made this study possible.

TABLE OF CONTENTS

LIST OF TABLES

LIST OF FIGURES

Figure Page

LIST OF SYMBOLS

a	distance from the front axle to the cab C. G.
b	distance from the rear axle to the vehicle C. G.
d	distance from kingpin to kingpin of the front axle
e	distance from kingpin to front wheel C. G.
F_s	force applied to tie-rod
F_{xi}	braking force on the tires
F_{yi}	tire side force
F_{zi}	tire normal load
g	gravity
h_c	height of tractor C. G.
h_{Fw}	height of fifth wheel
h_T	height of trailer C. G.
h_w	height of front wheel C. G.
$\bar{i}$	unit vector in the X direction
I_c	rotational inertia of the tractor
I_T	rotational inertia of the trailer
I_w	rotational inertia of front wheel
j	point of road contact for trailer tires
$\bar{j}$	unit vector in the Y direction
k	front wheel steering stabilizer spring constant
ℓ	distance to trailer C. G. from fifth wheel
m	distance to trailer axle from trailer C. G.

m_c	mass of tractor (cab)
m_T	mass of trailer
m_w	mass of front wheel
M	moment about fifth wheel
n	width of effective trailer axle
p_1	C. G. for the left front wheel
p_2	C. G. for the right front wheel
q	point of road contact for tractor rear tires
$\overline{R}_j$	position vector for right trailer tire point of contact
$\overline{R}_o$	position vector of the vehicle C. G. wrt the fixed axis system
$\overline{R}_{p_1}$	position vector for the left front wheel C. G.
$\overline{R}_{p_2}$	position vector for the right front wheel C. G.
$\overline{R}_{p_3}$	position vector for the tractor C. G.
$\overline{R}_q$	position vector for right rear tire point of contact
R_X	displacement of tractor C. G. wrt inertial reference down the road
R_Y	displacement of tractor C. G. wrt inertial reference across the road
s	distance from front wheel C. G. to tie-rod connection
α_F	front wheel slip angle
α_R	rear tractor wheel slip angle
α_T	trailer wheel slip angle
β	angle of front wheels wrt inertial reference
δ	angle of front wheels wrt tractor axis system
ε_F	front wheel heading angle
ε_R	rear tractor wheel heading angle
ε_T	trailer wheel heading angle

λ	angle of trailer wrt tractor axis system
σ	angle of trailer wrt inertial reference
θ	angle tractor makes wrt inertial reference

Subscripts

1	left front wheel
2	right front wheel
3	left rear tractor wheel
4	right rear tractor wheel
5	left trailer wheel
6	right trailer wheel

CHAPTER I

INTRODUCTION

The articulated vehicle has a prominent position in the present and future systems of rapid transportation of bulk cargos in this country. Because of the convenience of tractor-trailer combinations, larger and larger demands are being made of them. To satisfy these demands and to stay within the law, the tractors are being built smaller but more powerful, thus allowing the trailers to carry larger loads and still be under the weight limit. With ever increasing demands on rapid delivery, the stage is set for the effects of jackknifing to be greater than ever before.

Background

Dynamic response characteristics of articulated vehicles have become of increasing importance over the past twenty years. This is particularly because of the inherent stability problem of the tractor-trailer train. One of the first in-depth studies was performed by Jindra (2). In this analysis he developed the linearized equations of motion for a three degree-of-freedom model traveling at a constant speed in a steady, flat turn and analyzed the directional stability and control of the tractor and semi-trailer combination. He followed this with a linearized five degree-of-freedom tractor-trailer combination model with which he analyzed the lateral motion at a constant forward speed

with various fixed steering positions (3). Ellis (4) advanced Jindra's model with the inclusion of a suspension simulation derived by the use of Lagrange's equations. Mikulcik (5) developed a model of a tractor-semitrailer system that allowed both units to roll, yaw, pitch, and translate. He developed the equations of motion for both the linearized case and the nonlinearized case and compared results. It was found that some of the same conditions that jackknifed the nonlinearized model would not jackknife the linearized model; therefore, he concluded that linearized models should not be used for the investigation of jackknifing. Finally, Krauter and Wilson (6) developed an extension of Mikulcik's model that was nearly complete. It allowed translation, yaw, roll, and pitch of both tractor and semitrailer; lateral and fore-and-aft weight transfer; wheel dynamics, which included considering the effects of wheel slip, slip angle, vehicle speed, and tire load in the calculation of the tire forces. Also, the vehicle was maneuvered by a simulated driver who specified the front wheel steering angle and the brake torques. Methods of calculation of the above model were improved by Vincent and Krauter (7).

When the model development of articulated vehicles came into prominence, the idea of jackknife prevention generated a host of research studies. Leucht (8) analyzed a commercial tractor-semitrailer vehicle in a turn and subjected it to various brake applications including a load-sensitive brake-torque control. As mentioned by Marples (9), the general consensus in the industry was that the answer to jackknifing lay in load-proportional braking and not in fifth wheel devices. He documented several authorities that supported this opinion. In fact, he

stated that there was little room for confidence in the belief that a fifth wheel device would prevent jackknifing.

However, there have been many fifth wheel devices developed and placed on the market. Some were designed with sound engineering procedure, and some were developed through physical insight. Ordorica (10) described the "Mather Jackknife Control Unit" which is a damping device that was to replace the fifth wheel assembly and provide a maximum of 5000 foot-pounds torque. Keller (11) has devised a control unit that prevents the angle between the tractor and the trailer from exceeding 10°-15° by placing a piston so as to prevent rotation. It is engaged or disengaged from a control in the cab. Walsh and Cicchetti (12) developed a device that goes into effect as the brakes are applied. It prevents the angle between the tractor and the trailer from changing when the brakes are applied firmly.

In partial contrast to the opinions expressed in (9), Mikulcik (5) put forth the view that even if the fifth wheel devices are incapable of preventing jackknifing, they are capable of aiding in the prevention of jackknifing if properly constructed by allowing the driver more time to respond. Olsson (13) supported this opinion and this thesis will attempt to provide further evidence to support this opinion.

For tractor swing jackknifing to occur (i.e., when the tractor swings about the trailer) only three conditions need be present at moderately high speeds:

1. a large trailer mass relative to that of the tractor.
2. the fifth wheel under longitudinal (lengthwise) compression.
3. the tractor tires incapable of supplying enough side force to

develop a sufficiently large moment about the fifth wheel to counter the tractor inertial moment about the fifth wheel.

Step one above obviously will not be altered. Step two above is not subject to control in many cases of poor road condition or vehicle malfunction. Therefore, step three is the one that most of the anti-jackknifing groups are attacking. They are doing this using a multitude of different methods.

Because so many different methods of eliminating jackknifing are being devised, it was felt that an investigation of the characteristics of real and hypothetical fifth wheel anti-jackknifing devices should be made. In addition, it was convenient to include the front wheel steering stabilizer device of Turney's investigation (1) so as to prove the validity of the program developed during this study through comparison, and to determine the effect of such a device on an articulated vehicle.

The three major objectives of this study were:

1. To derive the equations of motion describing the dynamic response characteristics of a five degree-of-freedom, three-axle, articulated vehicle equipped with a front wheel steering stabilizer device and a fifth wheel anti-jackknifing device.

2. To develop the computer program necessary to solve numerically the above equations of motion utilizing all needed auxiliary equations.

3. To make a preliminary parametric study of the effects of a spring centered steering stabilizer device and a fifth wheel anti-jackknifing device on the dynamic response characteristics of a typical tractor-semi-trailer.

The results described within this document (or obtained from the program listed within this document) should not be relied upon

quantitatively without due regard to the assumptions made. The qualitative results, however, are considered to be correct as the assumptions were made rationally and with due respect to the information desired.

The part of this document concerning the spring centered steering stabilizer is a direct extension of Turney's Master of Science thesis (1) to articulated vehicles. Because of this, nothing should be mentioned pertaining to the steering stabilizer's background other than to refer the reader to (1).

Approach to the Problem

In the derivation of the equations of motion many simplifying assumptions were made. No frictional losses of any nature were considered. No subtle energy losses of any type were considered. The model of the articulated vehicle had no suspension. Only flat road surfaces were considered. The model's steering system had none of the normal characteristics other than the ability to change the heading angle of the front wheels. Where pairs of tires existed, the tire forces were assumed to be equal and to act at a point midway between the tires. The fifth wheel was modeled as being frictionless and was not allowed to transfer moment from the trailer to the tractor (i.e., it only transferred forces). Load shifts due to horizontal and lateral accelerations were accounted for in calculating the vertical forces acting on the tires. The model had five degrees of freedom.

A vector approach was used in the development of the equations of motion. The acceleration terms were derived in Chapter II and in the Appendices. Newton's Laws of Motion were used in conjunction with the acceleration terms to obtain the equations of motion.

A computer program was written and is described in Chapter III. There is an abbreviated flowchart of the computer program shown in Figure 16. The computer program utilized the Runge-Kutta 4th Order method of numerical integration and used subroutines for determining tire forces, coefficients of friction, steering forces, and fifth wheel device moments.

The results of the program are given in Chapter IV. The program was verified through four comparison cases. The tractor-semitrailer combination then was analyzed for the cases of:

1. Investigation of jackknifing with and without fifth wheel devices.

2. Investigation of the loss of maneuverability due to the fifth wheel devices.

3. Investigation of the response of the articulated vehicle with and without the spring centered front wheel stabilizer, and with and without the fifth wheel devices.

The summary, conclusions and recommendations of the research are given in Chapter V.

CHAPTER II

DERIVATIONS OF THE EQUATIONS

Equations of Motion

The equations of motion were derived by applying Newton's Laws of Motion to the typical tractor-trailer combination. Because rigid body motion was assumed there were six spatial degrees of freedom for each unit (i.e., tractor, trailer, left front wheel, and right front wheel) considered. After applying the assumption of planar motion, the number of degrees of freedom for each unit was reduced to three. Then applied were the constraints that the trailer and both front wheels must remain attached to the tractor and may only rotate about that point of attachment. The final restraint was that the front wheels were constrained to move through the same angle due to the tie-rod bond. This then reduced the model to a five degree-of-freedom system.

A moving body axis system with the origin located at the tractor center of gravity and referenced to an inertial axis system was used. Also, moving body axis system (1), (2) and (3) with their origins located at the centers of gravity of the left front wheel, right front wheel, and the trailer, respectively, were used and were referenced to the tractor (cab) moving body axis system.

Figure 1 shows the moving body axis system referenced to the vehicle. Figure 2 shows the method of sequentially referencing the various axis systems. Differentiation of the position vector twice with

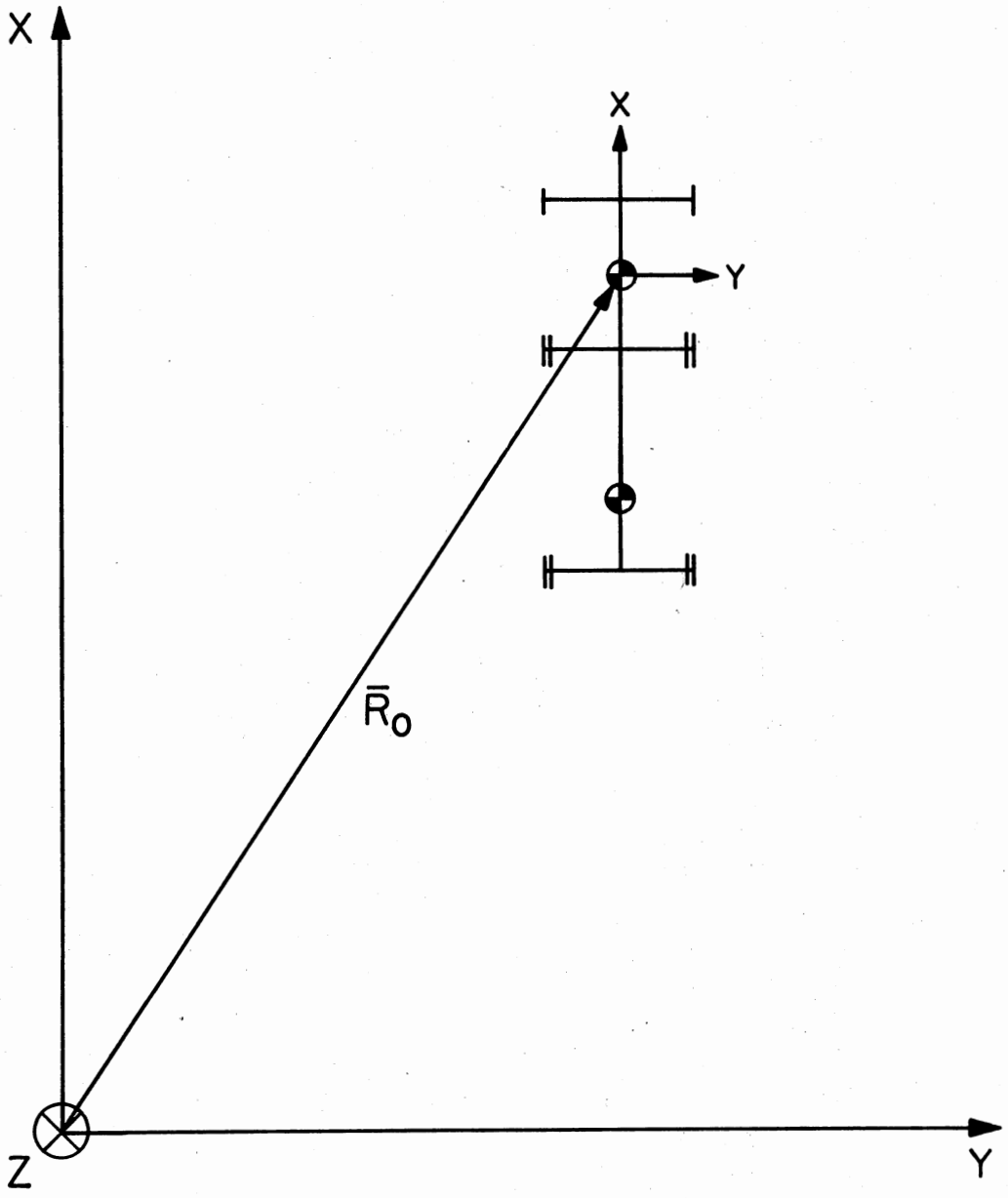

Figure 1. Moving Body Axis System Referenced to the Vehicle

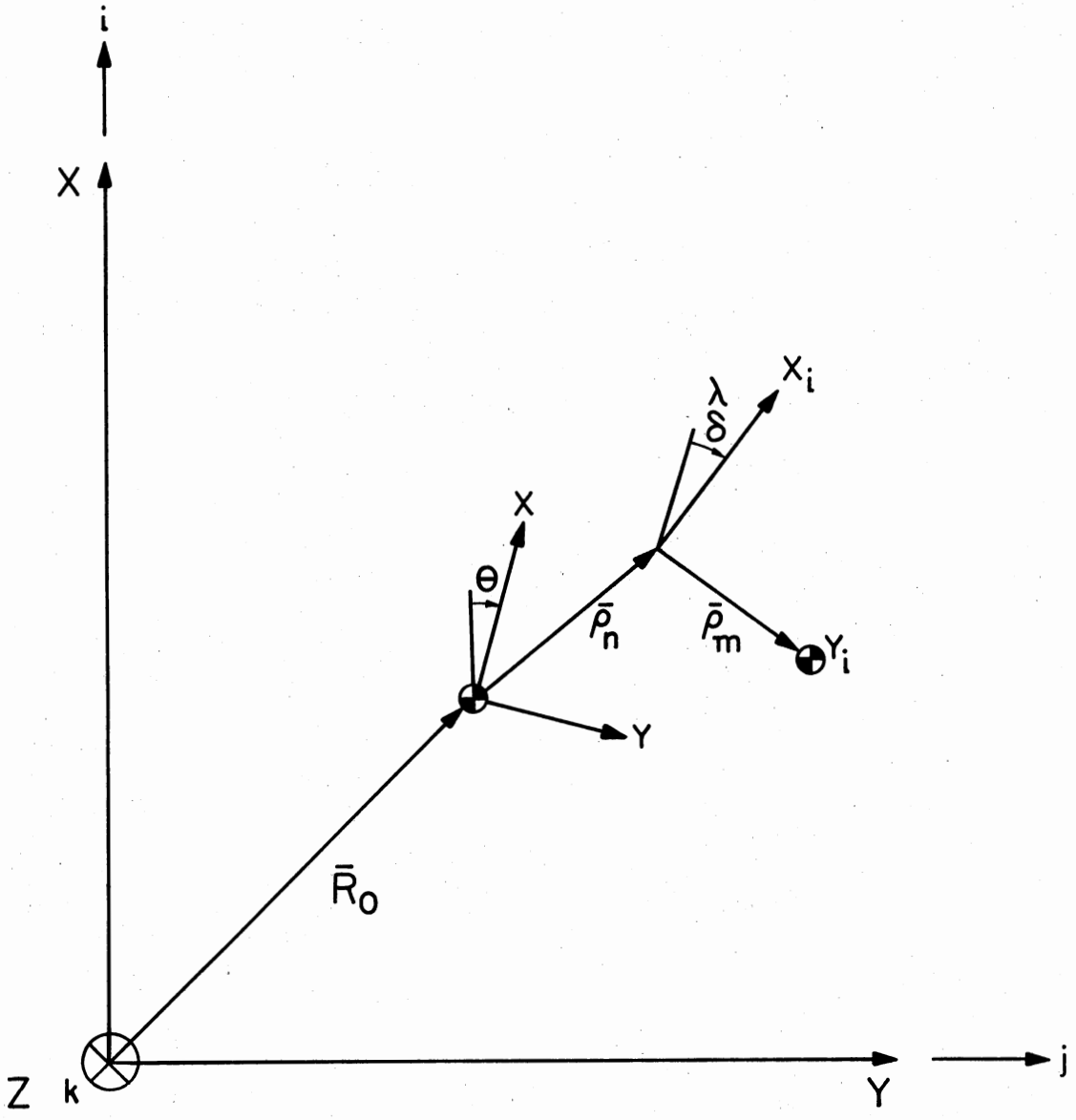

Figure 2. Wheel or Trailer Body Axis System
Referenced to Cab Body Axis System
Referenced to Inertial Axis System

respect to time yields the acceleration of the tractor center of gravity with respect to the inertial reference system:

$$\ddot{\bar{R}}_o = \ddot{R}_X \bar{i} + \ddot{R}_Y \bar{j} \tag{2.1}$$

Newton's Equations of Motion for this vehicle are:

$$m\ddot{R}_X = \Sigma F_X \tag{2.2}$$

$$m\ddot{R}_Y = \Sigma F_Y \tag{2.3}$$

$$I\ddot{\theta} = \Sigma M_{CG} \tag{2.4}$$

The forces are shown for the entire articulated vehicle in Figure 3. The braking forces act in the heading direction of the tires and are denoted as F_{xi}. The side forces act perpendicular to the braking forces through a point directly beneath the center of gravity of the wheel and are denoted as F_{yi}. The spring centered steering stabilizer causes a moment about the kingpin which opposes the front wheel steering angle. This moment is denoted as $K\delta$. The fifth wheel anti-jackknifing device causes a moment about the fifth wheel which opposes the tractor-trailer angle and is denoted as M.

Because the model studied consisted of four masses, it was necessary to develop the three equations of motion for each mass separately and then combine them through the constraint equations to obtain the final five equations completely describing the motion of the vehicle. The acceleration term for the tractor center of gravity is shown in Equation (2.1). The acceleration terms for the left front wheel ($\ddot{\bar{R}}_{p1}$) and the right front wheel ($\ddot{\bar{R}}_{p2}$) are developed in Appendix A and are shown below:

$$\ddot{\bar{R}}_{p1} = \ddot{\bar{R}}_o + [\ddot{\theta}d/2 - \dot{\theta}^2 a + \ddot{\beta} e\cos\delta - \dot{\beta}^2 e\sin\delta]\bar{i}\cos\theta$$

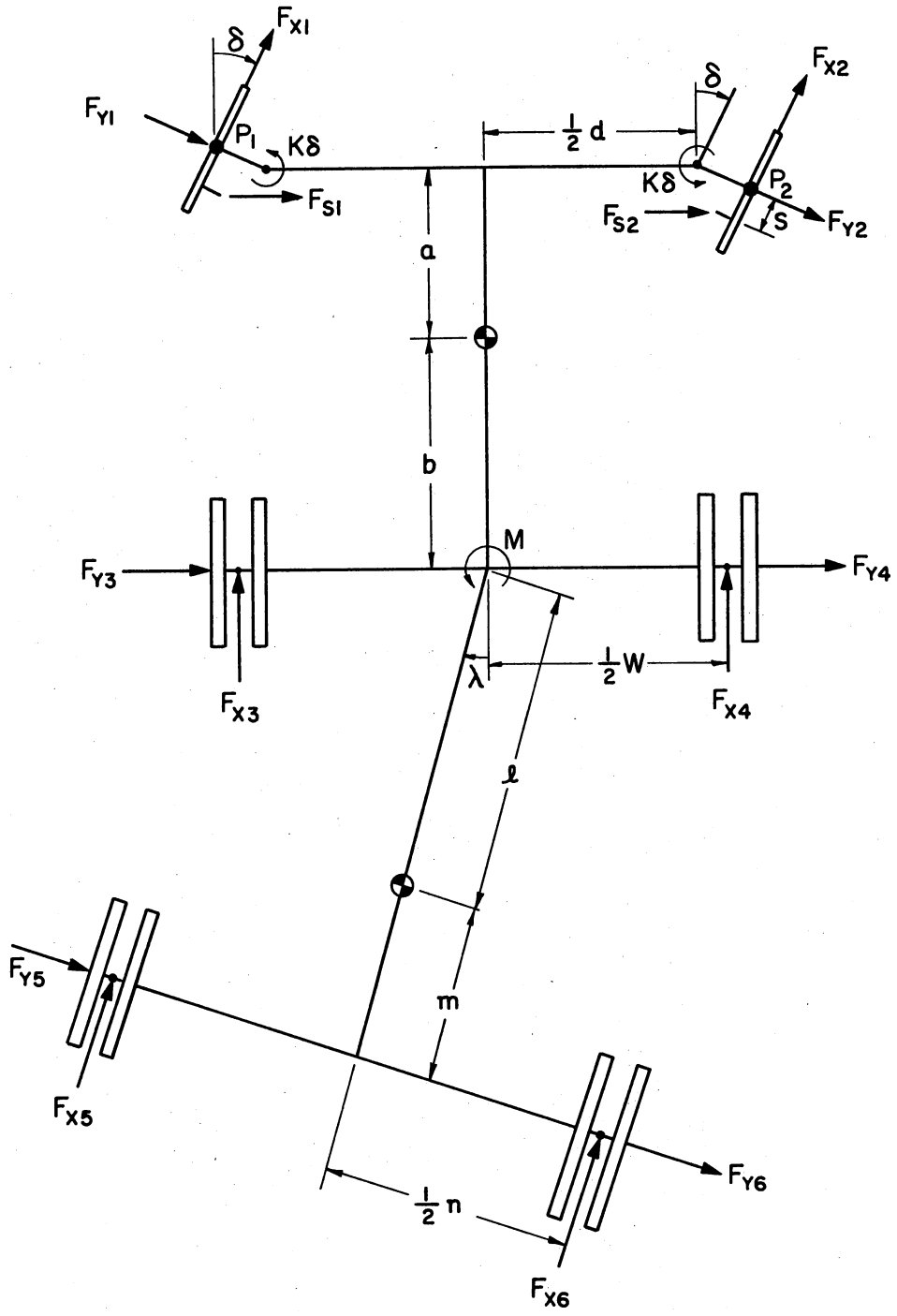

Figure 3. Diagram of the Forces (Internal and External) Acting on the Articulated Vehicle

$$+ [\ddot{\theta}d/2 - \dot{\theta}^2 a + \ddot{\beta}e\cos\delta - \dot{\beta}^2 e\sin\delta]\bar{j}\sin\theta$$

$$- [\ddot{\theta}a + \dot{\theta}^2 d/2 + \ddot{\beta}e\sin\delta + \dot{\beta}^2 e\cos\delta]\bar{i}\sin\theta$$

$$+ [\ddot{\theta}a + \dot{\theta}^2 d/2 + \ddot{\beta}e\sin\delta + \dot{\beta}^2 e\cos\delta]\bar{j}\cos\theta \qquad (2.5)$$

Similarly for the right front wheel:

$$\ddot{\bar{R}}_{p2} = \ddot{\bar{R}}_o$$

$$+ [-\ddot{\theta}d/2 - \dot{\theta}^2 a - \ddot{\beta}e\cos\delta + \dot{\beta}^2 e\sin\delta]\bar{i}\cos\theta$$

$$+ [-\ddot{\theta}d/2 - \dot{\theta}^2 a - \ddot{\beta}e\cos\delta + \dot{\beta}^2 e\sin\delta]\bar{j}\sin\theta$$

$$- [\ddot{\theta}a - \dot{\theta}^2 d/2 - \ddot{\beta}e\sin\delta - \dot{\beta}^2 e\cos\delta]\bar{i}\sin\theta$$

$$+ [\ddot{\theta}a - \dot{\theta}^2 d/2 - \ddot{\beta}e\sin\delta - \dot{\beta}^2 e\cos\delta]\bar{j}\cos\theta \qquad (2.6)$$

The acceleration term for the trailer center of gravity ($\ddot{\bar{R}}_{p3}$) is developed in Appendix B and is given by:

$$\ddot{\bar{R}}_{p3} = \ddot{\bar{R}}_o$$

$$+ [\dot{\theta}^2 b + \ddot{\sigma}\ell\sin\lambda + \dot{\sigma}^2 \ell\cos\lambda]\bar{i}\cos\theta$$

$$+ [\dot{\theta}^2 b + \ddot{\sigma}\ell\sin\lambda + \dot{\sigma}^2 \ell\cos\lambda]\bar{j}\sin\theta$$

$$- [-\ddot{\theta}b - \ddot{\sigma}\ell\cos\lambda + \dot{\sigma}^2 \ell\sin\lambda]\bar{i}\sin\theta$$

$$+ [-\ddot{\theta}b - \ddot{\sigma}\ell\cos\lambda + \dot{\sigma}^2 \ell\sin\lambda]\bar{j}\cos\theta \qquad (2.7)$$

After having derived the acceleration terms for the four masses, Newton's Equations of Motion were applied to the front wheel masses. Free-body diagrams of the front wheels are shown in Figures 4 and 5. The derivation of the equations of motion are shown in Appendix C. After applying the tie-rod constraint, the equations combine and become:

$$\ddot{\beta} = (I_w + m_w e^2)^{-1} \begin{bmatrix} -k\delta - \frac{1}{2} F_s s\cos\delta + \frac{1}{2} e(F_{x1} - F_{x2}) \\ -m_w ed/2(\ddot{\theta}\cos\delta + \dot{\theta}^2\sin\delta) \end{bmatrix} \qquad (2.8)$$

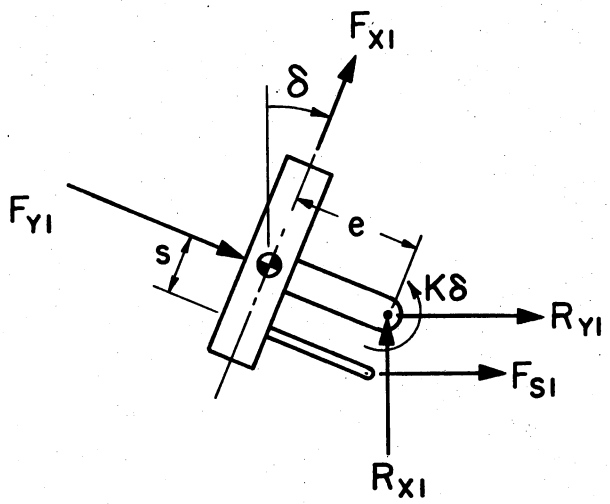

Figure 4. Forces Acting on the Left Front Wheel

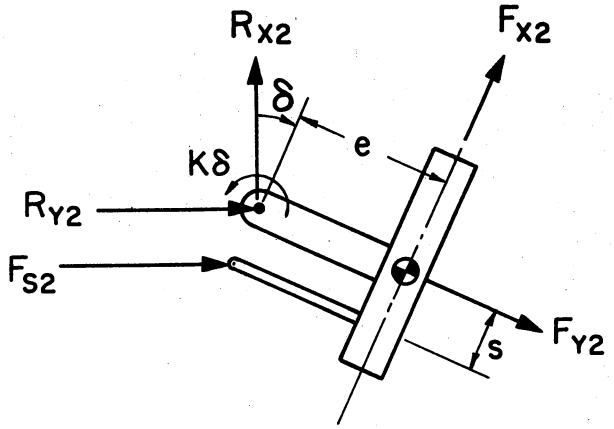

Figure 5. Forces Acting on the Right Front Wheel

The next equation of motion determined was that of the trailer rotation $\ddot{\sigma}$. Again, Newton's Equations of Motion were applied. The free-body diagram of the trailer is shown in Figure 6. The derivation of this equation of motion is shown in Appendix D and by letting $D_1 = 1/(I_T + m_T\ell^2)$ it is shown that:

$$\ddot{\sigma} = D_1 \left[-M - (F_{y5} + F_{y6})(m + \ell) + (F_{x5} - F_{x6})n/2 \right.$$
$$\left. -m_T\ell \left[\begin{array}{l} (\ddot{R}_X\cos\theta + \ddot{R}_Y\sin\theta)\sin\lambda \\ -(-\ddot{R}_X\sin\theta + \ddot{R}_Y\cos\theta)\cos\lambda \\ +b(\dot{\theta}^2\sin\lambda + \ddot{\theta}\cos\lambda) \end{array} \right] \right] \qquad (2.9)$$

By applying the constraint assumptions mentioned earlier through substitution methods, the final three equations of motion are derived in Appendices E, F and G using the free-body diagram of Figure 7. By allowing the simple substitution of $D_2 = \cos\theta/(m_c + 2m_w + m_T)$ and $D_3 = \sin\theta/(m_c + 2m_w + m_T)$, the equation of motion for $\ddot{R}_X$ is given by:

$$\ddot{R}_X = D_2 \left[\begin{array}{l} (F_{x1} + F_{x2})\cos\delta + (F_{x3} + F_{x4}) + (F_{x5} + F_{x6})\cos\lambda \\ -(F_{y1} + F_{y2})\sin\delta \qquad\qquad - (F_{y5} + F_{y6})\sin\lambda \\ +2m_w a\dot{\theta}^2 - m_T(b\dot{\theta}^2 + \ell\ddot{\sigma}\sin\lambda + \ell\dot{\sigma}^2\cos\lambda \end{array} \right]$$
$$+ D_3 \left[\begin{array}{l} -(F_{x1} + F_{x2})\sin\delta \qquad\qquad -(F_{x5} + F_{x6})\sin\lambda \\ -(F_{y1} + F_{y2})\cos\delta - (F_{y3} + F_{y4}) - (F_{y5} + F_{y6})\cos\lambda \\ +2m_w a\ddot{\theta} + m_T(-b\ddot{\theta} - \ell\ddot{\sigma}\cos\lambda + \ell\dot{\sigma}^2\sin\lambda) \end{array} \right]$$

(2.10)

Similarly,

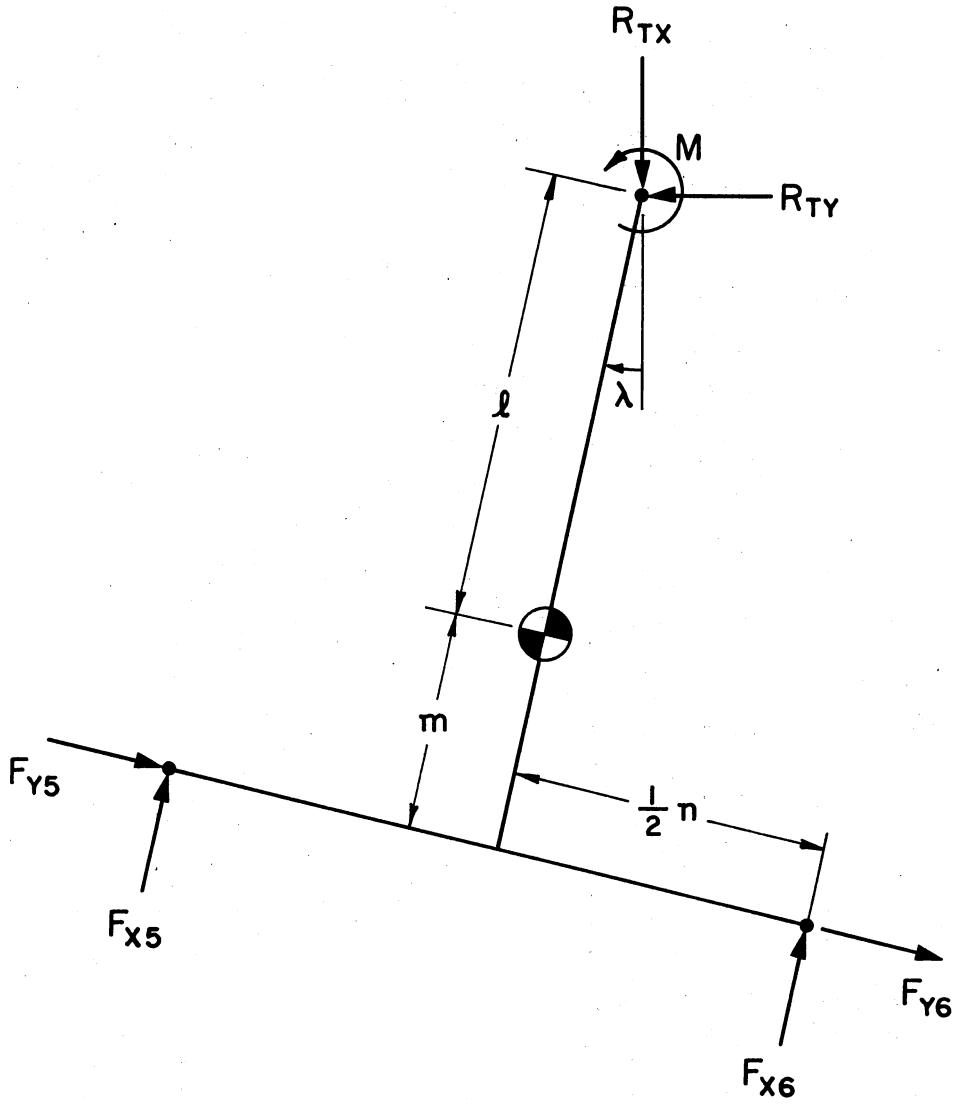

Figure 6. Free-Body Diagram for the Trailer

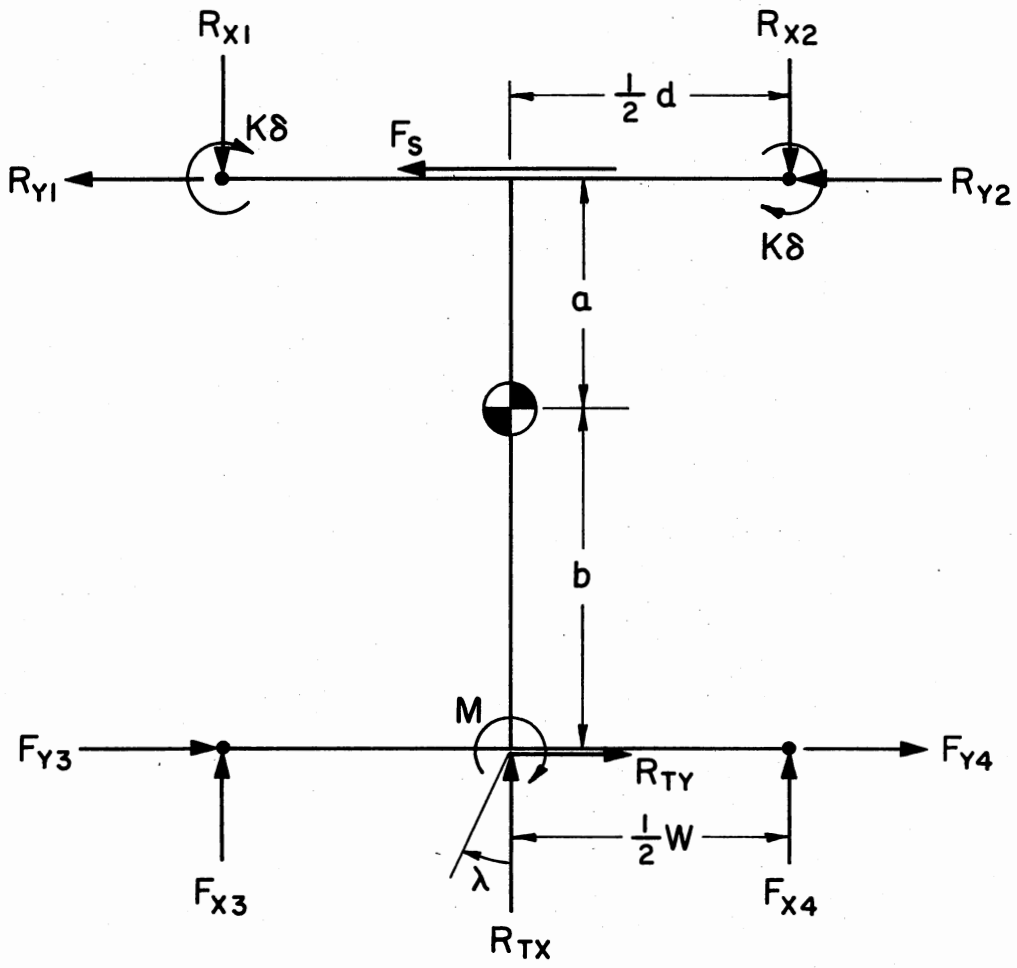

Figure 7. Free-Body Diagram for the Vehicle (Less the Front Wheels and Trailer)

$$\ddot{R}_Y = D_2 \begin{bmatrix} (F_{x1} + F_{x2})\sin\delta & + (F_{x5} + F_{x6})\sin\lambda \\ +(F_{y1} + F_{y2})\cos\delta + (F_{y3} + F_{y4}) + (F_{y5} + F_{y6})\cos\lambda \\ -2m_w a\ddot{\theta} - m_T(-b\ddot{\theta} - \ell\ddot{\sigma}\cos\lambda + \ell\dot{\sigma}^2\sin\lambda) \end{bmatrix}$$

$$+ D_3 \begin{bmatrix} (F_{x1} + F_{x2})\cos\delta + (F_{x3} + F_{x4}) + (F_{x5} + F_{x6})\cos\lambda \\ -(F_{y1} + F_{y2})\sin\delta & - (F_{y5} + F_{y6})\sin\lambda \\ +2m_w a\dot{\theta}^2 - m_T(b\dot{\theta}^2 + \ell\ddot{\sigma}\sin\lambda + \ell\dot{\sigma}^2\cos\lambda) \end{bmatrix}$$

(2.11)

Finally, by letting $D_4 = 1/\{I_c + 2m_w(a^2 + [d/2]^2 + m_T b^2\}$, the equation of motion for $\ddot{\theta}$ is:

$$\ddot{\theta} = -aD_4 \begin{bmatrix} -(F_{x1} + F_{x2})\sin\delta - (F_{y1} + F_{y2})\cos\delta \\ + m_w(-2\ddot{R}_X\sin\theta + 2\ddot{R}_Y\cos\theta) \end{bmatrix}$$

$$-bD_4 \begin{bmatrix} (F_{x5} + F_{x6})\sin\lambda + (F_{y3} + F_{y4}) + (F_{y5} + F_{y6})\cos\lambda \\ -m_T \begin{bmatrix} -\ddot{R}_X\sin\theta + \ddot{R}_Y\cos\theta \\ -\ell\ddot{\sigma}\cos\lambda + \ell\dot{\sigma}^2\sin\lambda \end{bmatrix} \end{bmatrix}$$

$$-\frac{dD_4}{2} \begin{bmatrix} -(F_{x1} - F_{x2})\cos\delta + (F_{y1} - F_{y2})\sin\delta \\ +2m_w(e\cos\ddot{\beta} - e\dot{\beta}^2\sin\delta) \end{bmatrix}$$

$$+D_4 \quad [M + 2k\delta + w/2(F_{x3} - F_{x4})] \qquad (2.12)$$

The equations of motion are now complete (i.e., Equations (2.8, 2.9, 2.10, 2.11, 2.12)). Because the tire side forces and the braking forces were a function of the normal load on the tire and the slip angle, these were the next equations developed.

Equations of Tire Normal Loads and Slip Angles

Figure 8 shows the forces involved causing a weight shift on the axles during a forward acceleration of the articulated vehicle. Figure 9 shows the free-body diagram of the tractor with the wheels attached. This meant that there was an assumption of no front wheel angle change which certainly would not affect the normal loads significantly. To determine the axial loads on the tractor axles a simple summation of moments about the y-axis through the point of tire contact with the road for both the front and rear axles was performed. This involved trailer reactions, however, so similar summations of moments about the y_3-axis through the fifth wheel and through the point of tire contact with the road were required before the loads on the axles could be determined. The complete derivation is given in Appendix H.

Letting $D_5 = 1/(a+b)$, the load on the front axle is given by:

$$\begin{aligned} Z_1 = {} & 2m_w g + m_c g(bD_5) \\ & + (h_{Fw}D_5)\left[-(F_{y5} + F_{y6})\sin\lambda + (F_{x5} + F_{x6})\cos\lambda\right. \\ & \left. - m_T\left[\ddot{R}_X\cos\theta + \ddot{R}_Y\sin\theta \right.\right. \\ & \left.\left. + b\dot{\theta}^2 + \ell\ddot{\sigma}\sin\lambda + \ell\dot{\sigma}^2\cos\lambda\right]\right] \\ & - (m_w h_w D_5)2[\ddot{R}_X\cos\theta + \ddot{R}_Y\sin\theta - a\dot{\theta}^2] \\ & - (m_c h_c D_5)[\ddot{R}_X\cos\theta + \ddot{R}_Y\sin\theta] \end{aligned} \tag{2.13}$$

Letting $D_6 = 1/(m+\ell)$, the load on the tractor rear axle is given by:

$$Z_2 = m_c g(aD_5) + m_T g(mD_6) - (h_{Fw}D_6)(F_{x5} + F_{x6})$$

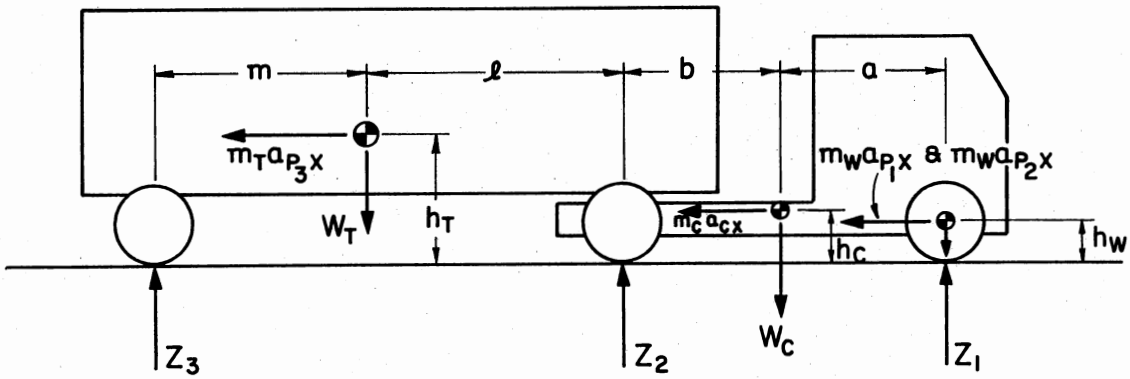

Figure 8. Normal Forces and Weight Transfer During Forward Acceleration of the Articulated Vehicle

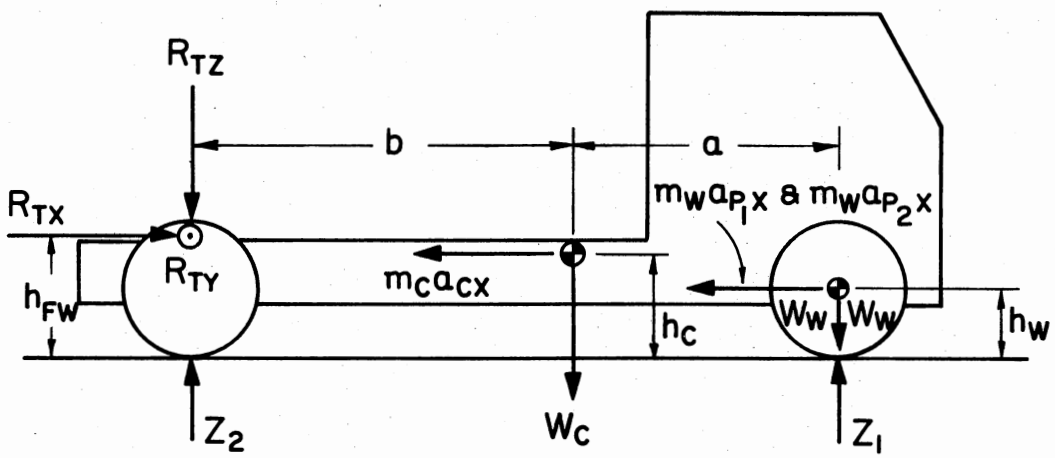

Figure 9. Applied Forces and Weight Transfer During Forward Acceleration of the Cab

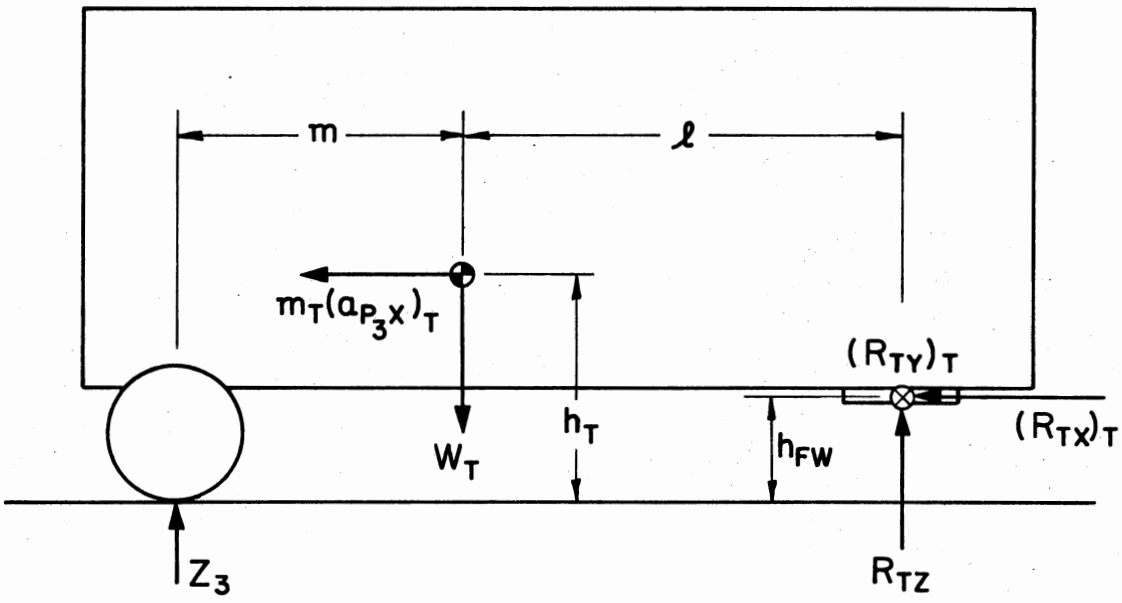

Figure 10. Applied Forces and Weight Transfer During Forward Acceleration of the Trailer

$$- (h_{Fw}D_5)\left[-(F_{y5} + F_{y6})\sin\lambda + (F_{x5} + F_{x6})\cos\lambda\right.$$
$$\left.-m_T\left[\ddot{R}_X\cos\theta + \ddot{R}_Y\sin\theta\right.\right.$$
$$\left.\left. + b\dot{\theta}^2 + \ell\ddot{\sigma}\sin\lambda + \ell\dot{\sigma}^2\cos\lambda\right]\right]$$
$$+ [m_T(h_{Fw} - h_T)D_6]\left[(\ddot{R}_X\cos\theta + \ddot{R}_Y\sin\theta)\cos\lambda\right.$$
$$+ (-\ddot{R}_X\sin\theta + \ddot{R}_Y\cos\theta)\sin\lambda$$
$$\left. + (b\dot{\theta}^2)\cos\lambda - (b\ddot{\theta})\sin\lambda + \ell\dot{\sigma}^2\right]$$
$$+ (m_c h_c D_5)[\ddot{R}_X\cos\theta + \ddot{R}_Y\sin\theta]$$
$$+ (m_w h_w D_5)2[\ddot{R}_X\cos\theta + \ddot{R}_Y\sin\theta - a\dot{\theta}^2] \qquad (2.14)$$

The normal load on the trailer axle is given by:

$$Z_3 = D_6[(F_{x5} + F_{x6})h_{Fw} + m_T g(\ell)]$$
$$+ [m_T(h_T - h_{Fw})D_6]\left[(\ddot{R}_X\cos\theta + \ddot{R}_Y\sin\theta)\cos\lambda\right.$$
$$+ (-\ddot{R}_X\sin\theta + \ddot{R}_Y\cos\theta)\sin\lambda$$
$$\left. + b\dot{\theta}^2\cos\lambda - b\ddot{\theta}\sin\lambda + \ell\dot{\sigma}^2\right] \qquad (2.15)$$

The equations for determining the loads on the axles have been completed. These equations were next used in determining the specific loads on the tires. The variable term used was F_{Zi}. Figures 11, 12 and 13 show the forces involved on the three axles under consideration during a lateral acceleration (or weight shift). The normal loads were determined by summing moments about the x-axis through points A and B or the $(x)_T$-axis through point C and applying the requirement that the summation of forces in the vertical direction must be equal to zero. For a complete derivation see Appendix I. The equations, letting $D_7 = 1/(d + 2e)$, are as follows:

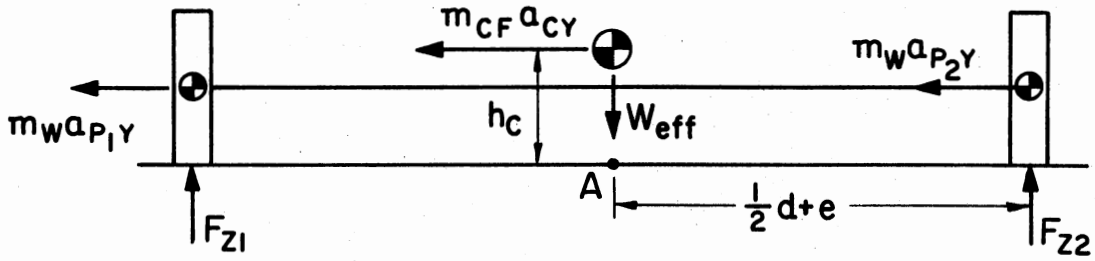

Figure 11. Cab Front Axle Diagram

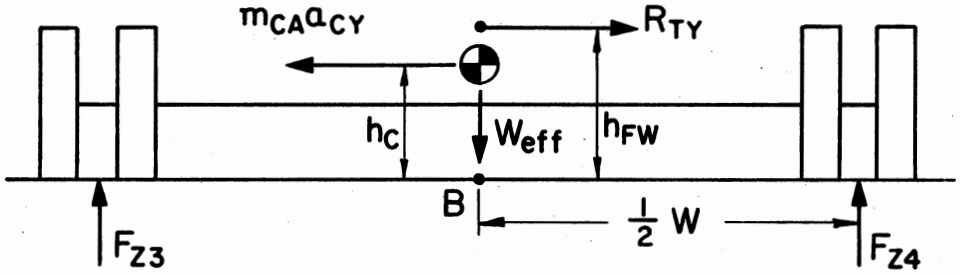

Figure 12. Cab Rear Axle Diagram

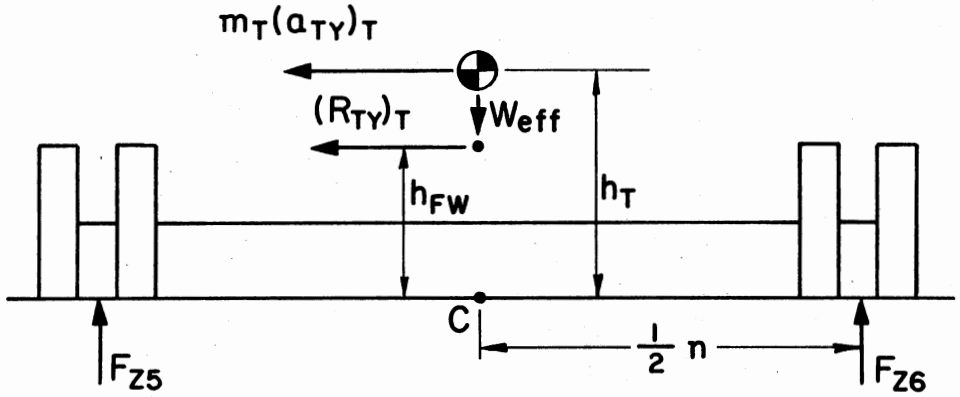

Figure 13. Trailer Axle Diagram

$$F_{Z1} = (m_w h_w D_7)2[-\ddot{R}_X \sin\theta + \ddot{R}_Y \cos\theta + a\ddot{\theta}]$$

$$+ \frac{1}{2} Z_1$$

$$+ (m_c h_c D_7)(bD_5)[-\ddot{R}_X \sin\theta + \ddot{R}_Y \cos\theta] \tag{2.16}$$

$$F_{Z2} = Z_1 - F_{z1} \tag{2.17}$$

$$F_{Z3} = -(h_{Fw}/w) \left[(F_{y5} + F_{y6})\cos\lambda + (F_{x5} + F_{x6})\sin\lambda \right.$$

$$\left. -m_T \left[-\ddot{R}_X \sin\theta + \ddot{R}_Y \cos\theta \right. \right.$$

$$\left. \left. -b\ddot{\theta} - \ell\ddot{\sigma}\cos\lambda + \ell\dot{\sigma}^2 \sin\lambda \right] \right]$$

$$+ (m_c h_c/w)(aD_5)[-\ddot{R}_X \sin\theta + \ddot{R}_Y \cos\theta]$$

$$+ \frac{1}{2} Z_2 \tag{2.18}$$

$$F_{Z4} = Z_2 - F_{Z3} \tag{2.19}$$

$$F_{Z5} = (h_{Fw}/n) \left[(F_{y5} + F_{y6}) + m_T \ell\ddot{\sigma} \right.$$

$$\left. +m_T \sin\lambda \ (\ddot{R}_X \cos\theta + R_Y \sin\theta + b\dot{\theta}^2) \right.$$

$$\left. -m_T \cos\lambda \ (-\ddot{R}_X \sin\theta + \ddot{R}_Y \cos\theta - b\ddot{\theta}) \right]$$

$$+ (m_T h_T/n) \left[-\ell\ddot{\sigma} - \sin\lambda(\ddot{R}_X \cos\theta + \ddot{R}_Y \sin\theta + b\dot{\theta}^2) \right.$$

$$\left. + \cos\lambda(-\ddot{R}_X \sin\theta + \ddot{R}_Y \cos\theta - b\ddot{\theta}) \right]$$

$$+ \frac{1}{2} Z_3 \tag{2.20}$$

$$F_{z6} = Z_3 - F_{z5} \tag{2.21}$$

Equations (2.13) through (2.21) completely describe the change in normal loads due to acceleration. As mentioned before, the braking forces and tire side forces were a function of the slip angle as well as normal load; therefore, the slip angles were also calculated.

The procedure was very similar for all three axles. The heading angles were defined with respect to the inertial reference and a clockwise rotation was chosen to be positive. The velocity vector angle was then calculated using the arctangent of the two component velocities with respect to the inertial reference. This calculation assumed that counterclockwise was the positive rotation. Due to the difference in sign conventions a simple addition gave the difference between the two angles which is the definition of slip angle. A complete derivation is given in Appendix J. The three slip angle equations were given by:

$$\alpha_F = \varepsilon_F + \tan^{-1}\left[\frac{\dot{R}_X + \dot{\theta}(d/2\cos\theta - a\sin\theta) + \dot{\beta}e\cos\beta}{\dot{R}_Y + \dot{\theta}(a\cos\theta + d/2\sin\theta) + \dot{\beta}e\sin\beta}\right] \tag{2.22}$$

$$\alpha_R = \varepsilon_R + \tan^{-1}\left[\frac{\dot{R}_X + \dot{\theta}(b\sin\theta - w/2\cos\theta)}{\dot{R}_Y + \dot{\theta}(-b\cos\theta - w/2\sin\theta)}\right] \tag{2.23}$$

$$\alpha_T = \varepsilon_T + \tan^{-1}\left[\frac{\dot{R}_X + \dot{\theta}b\sin\theta + \dot{\sigma}\{(\ell+m)\sin\sigma - n/2\cos\sigma\}}{\dot{R}_Y - \dot{\theta}b\cos\theta + \dot{\sigma}\{-(\ell+m)\cos\sigma - n/2\sin\sigma\}}\right] \tag{2.24}$$

This completes all of the equations used to describe the motion of the vehicle. The next chapter shows the development of the computer program to solve these equations.

CHAPTER III

DEVELOPMENT OF THE COMPUTER PROGRAM

A computer program was written to solve the equations of motion and the auxiliary equations of the preceding chapter. The computer used was an IBM 360/65. In the program the numerical integration technique used was the fourth-order Runge-Kutta method (14). The steering force was expressed as a function of state variables and calculated in the subroutine STEER. The fifth wheel moment was expressed as a function of state variables and calculated in the subroutine MOMENT. The braking forces and tire side forces were calculated in the subroutine FXFY and then modified according to the friction ellipse, if necessary.

As specified in detail for each problem in Chapter IV, the steering force and fifth wheel moment were stated as functions of state variables; therefore, the calculations were quite simple and not worth discussing here. The side forces and braking forces of the tires were functions of the axial and tire normal forces; therefore, Equations (2.13) through (2.21) were the first ones evaluated in the subroutine FXFY. Because the above mentioned forces were also a function of slip angle, Equations (2.22) through (2.24) were evaluated next in the tire forces subroutine.

Now that the tire normal forces and slip angles were defined, the tire side forces were interpolated for in the subroutine SEARCH if the slip angle was less than fourteen degrees (i.e., the angle at which the

tire is assumed to slip completely). The values of Figure 14 were placed in the subroutine SEARCH as the table for interpolation.

The subroutine SEARCH could not be used when the wheels were locked or the slip angle went beyond fourteen degrees. A simple method of friction coefficient multiplied by normal force had to be used instead. The friction coefficients were determined in the subroutine CIRCMU by entering with tire velocity and whether or not the wheels were locked. The table values are shown in Table I as obtained from Reference (6). The braking forces were also calculated by multiplying the appropriate friction coefficient by the tire normal load.

The tire side forces and the braking forces were calculated but the vector summation of these two forces sometimes produced an effective force that was larger than the maximum possible. That was why the friction ellipse of Figure 15 was needed (6). It is assumed in the construction of the friction ellipse that the distance from the origin to the ellipse represents the maximum possible tire-road force. For example, if a braking force were calculated to be as large as point A and a corresponding side force were calculated to be as large as point B, then the vector summation of the two would lie at point C, clearly outside the ellipse. What would transpire at this time is that the side force would be reduced to the value B' for further calculations. The shape of the friction ellipse is that the major axis is twice the normal load times the maximum unlocked coefficient of friction for the specific speed and the minor axis is twice the normal load times the maximum locked coefficient of friction for the specific speed (i.e., the friction ellipse changes shape with speed). If the vector summation of the tire forces

TABLE I

LOCKED AND UNLOCKED COEFFICIENTS OF FRICTION

Speed (ft/sec)	Locked Wheel Coefficient	Unlocked Wheel Coefficient
0.0	1.000	1.000
14.7	.720	1.000
29.3	.660	.925
44.0	.600	.850
58.7	.540	.775
73.3	.480	.700
88.0	.420	.625
102.7	.360	.550

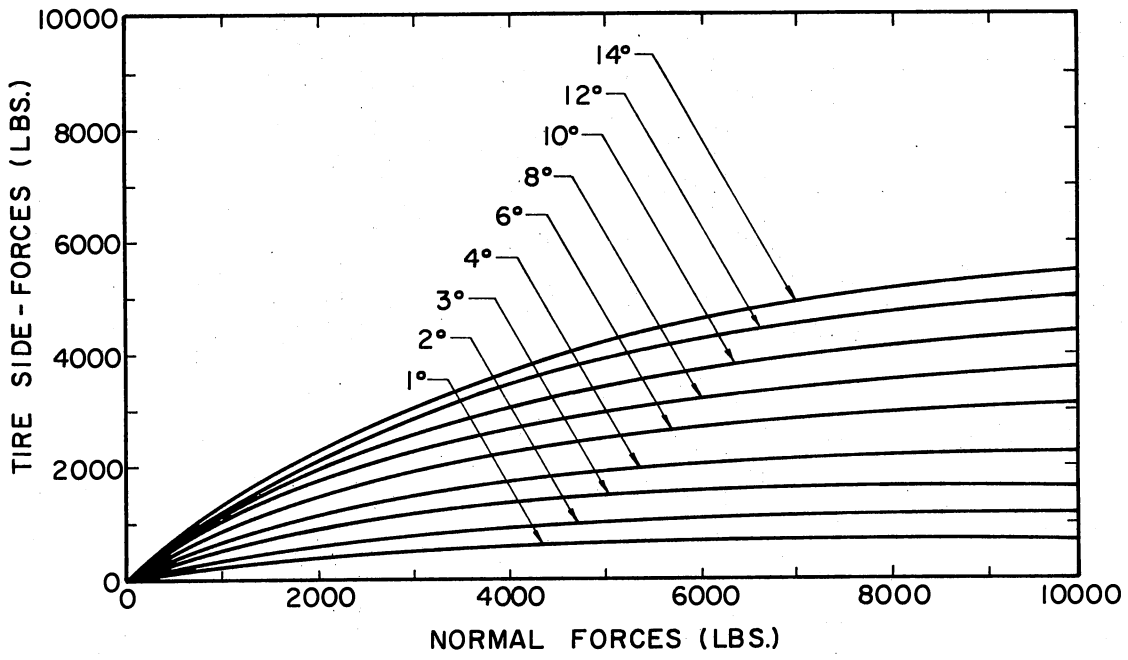

Figure 14. Graph of Tire Side-Forces Versus Normal Forces and Slip Angles

$FX_{MAX} = \mu_{MAX} N$

$FY_{MAX} = \mu_{MIN} N$

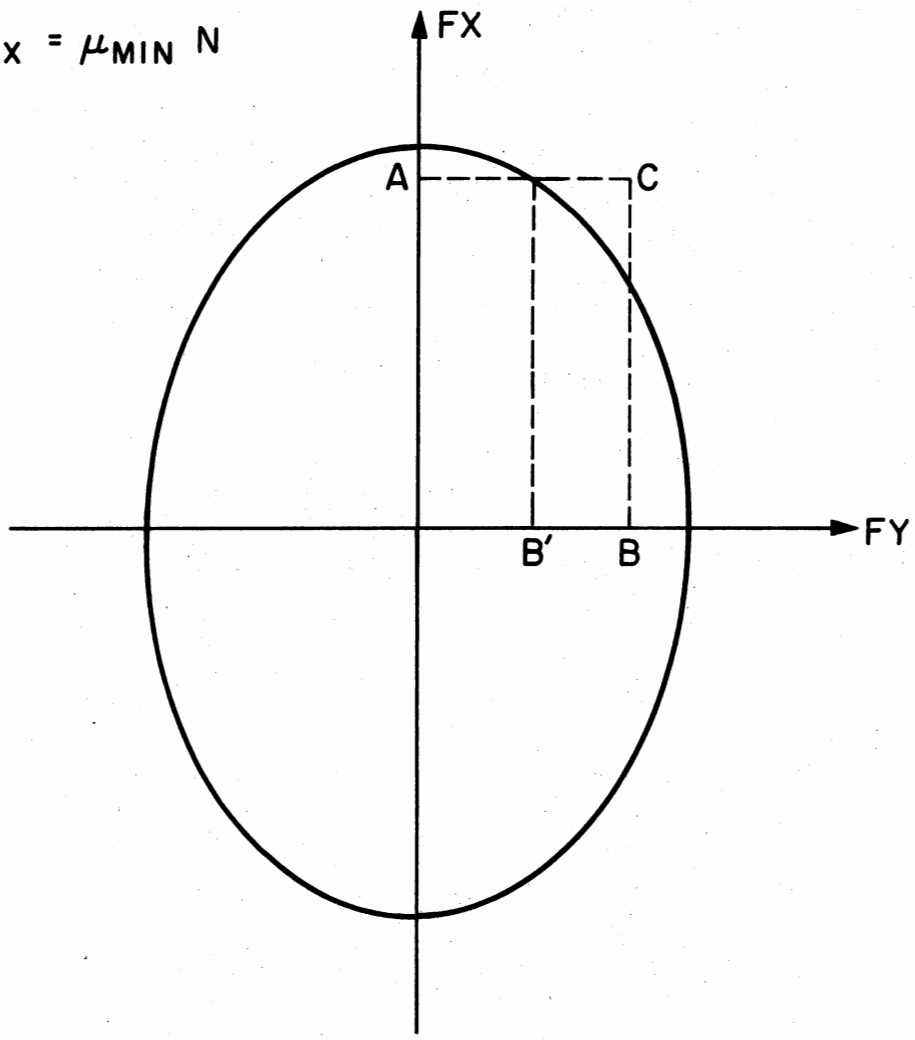

Figure 15. Friction Ellipse

lies inside the friction ellipse, then the braking force and the tire side force are independent.

The tire forces at this point had been completely defined for the next iteration. The state variables were then reinitialized and another iteration was calculated. A brief flow chart of the program is shown in Figure 16.

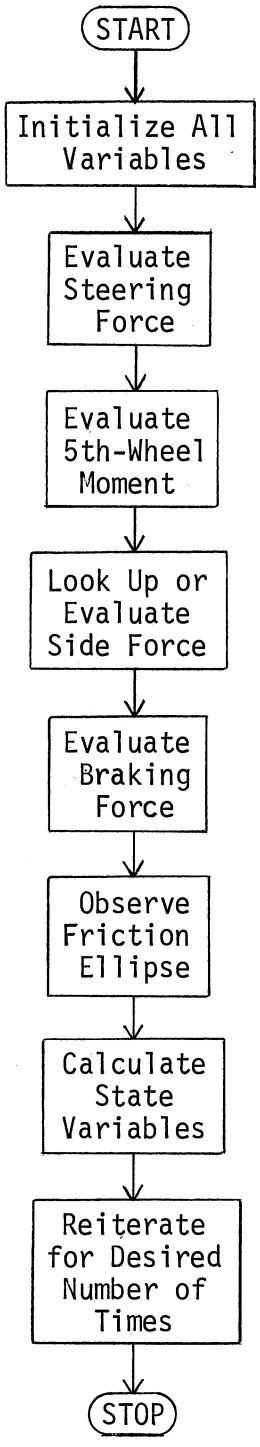

Figure 16. Flowchart of Computer Program

CHAPTER IV

NUMERICAL RESULTS

Verification of the Program

After the writing of the computer program it was verified through several different methods. These were comparison with an exact analytical solution, comparison of numerical results with those obtained by another computer program, and comparison of results obtained with those to be physically expected. In all cases of comparison "short cuts" were not used if at all possible. This allowed a more thorough checking of the program. Unfortunately, it also allowed small differences to appear that were due entirely to differences in basic assumptions and not to programming errors.

The first case used for verification was that of constant braking of the trailer wheels. Figure 17 shows both the numerical and analytical solutions for forward distance traveled as a function of time. The braking force applied was a total of -7000 pounds. The initial velocity was 88 feet per second and all other state variables were zero. The truck data used were that of set 2 in Table II. The computing increment was .125 seconds. The acceleration determined analytically was -5.10 feet per second per second and the acceleration determined numerically was -5.14 feet per second per second. The stopping times were identical at 17.4 seconds. The distances traveled differed by only 0.65 percent (i.e., 770 feet analytically as compared to 775 feet numerically). All state

TABLE II

TRUCK DATA

Item	Set 1	Set 2	Units
MW	9.32	10.50	$lb\text{-}sec^2/ft$
MC	466.00	416.00	$lb\text{-}sec^2/ft$
MT	0	935.00	$lb\text{-}sec^2/ft$
IW	25.00	6.81	$ft\text{-}lb\text{-}sec^2$
IC	6,000.00	10,300.00	$ft\text{-}lb\text{-}sec^2$
IT	83,500.00	83,500.00	$ft\text{-}lb\text{-}sec^2$
A	4.00	5.50	ft
B	6.00	6.25	ft
D	6.00	6.00	ft
E	.66	.404	ft
S	.75	.755	ft
G	32.20	32.20	ft/sec^2
W	7.00	8.00	ft
L	18.00	18.00	ft
M	12.00	12.00	ft
N	8.00	8.00	ft
HW	1.75	1.75	ft
HC	4.00	3.00	ft
HFW	3.50	3.50	ft
HT	6.00	6.00	ft

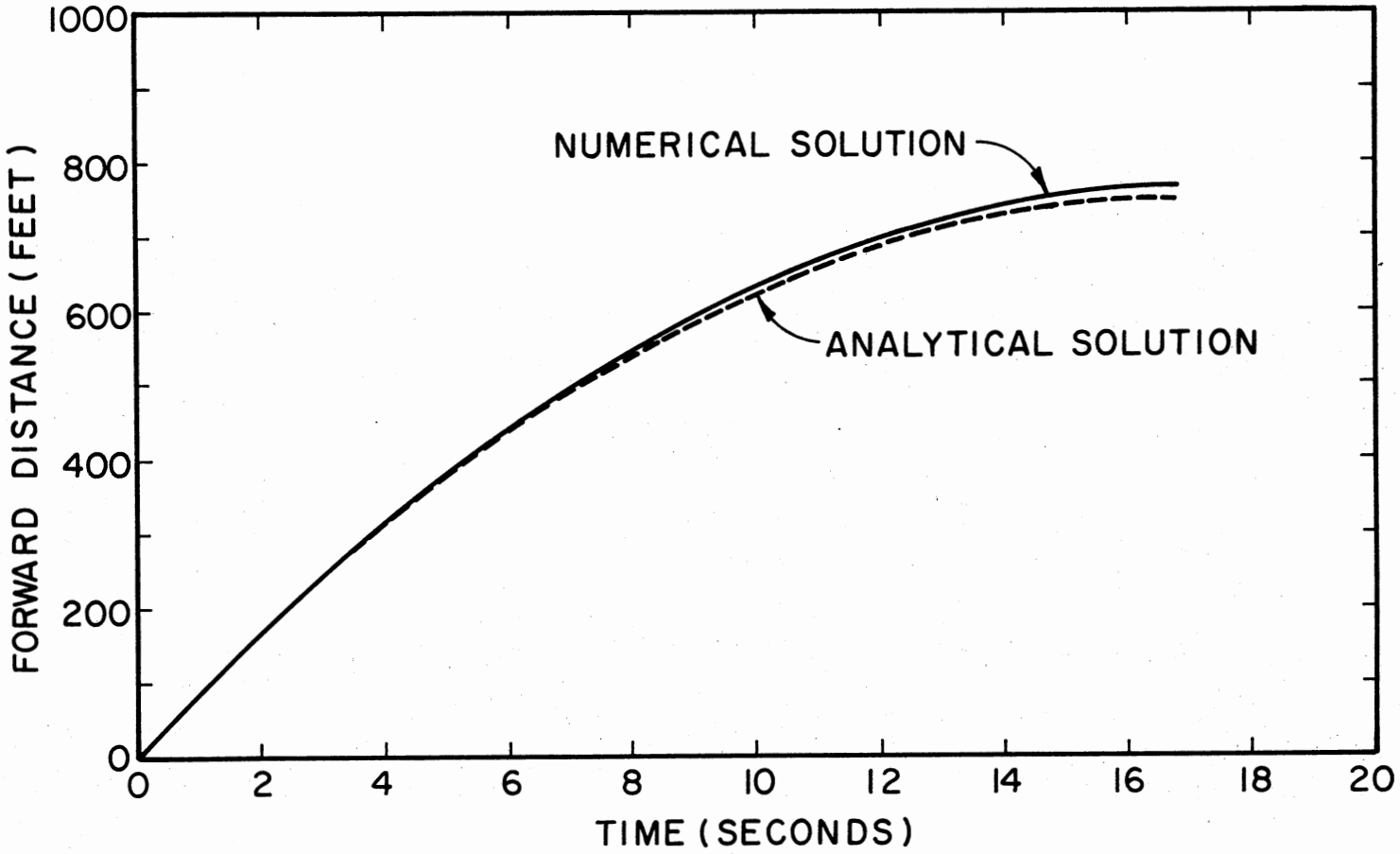

Figure 17. Comparison of Numerical and Analytical Solutions for Braking Results

variables other than those associated with forward motion remained identically zero as expected. This clearly showed a favorable comparison and allowed less room for program criticism within two significant digits.

The second case of comparison utilized results obtained by Turney (1) with his four degrees-of-freedom model. Figure 18 shows some of the results obtained from both programs. In these results the front wheel steering angle is shown as a function of time. The truck data used were that of set 1 in Table II. This series of program runs used a computing increment of .01 seconds because of numerical stability considerations. A numerical instability was recognized in this case as abnormally large values of the angles, displacements, and tire normal loads. These large values decreased as the computing increment was decreased until the increment of .01 seconds was reached, at which point the values leveled out. This was typical of the method used to determine the proper computing increment. The reference program used a computing increment of .125 seconds. A steering force (force at the tie rod) of 20 pounds was applied at t = 2 seconds for a period of 1 second. Subsequently a steering force of -40 pounds was applied at t = 5.5 seconds for a period of 1 second. A final steering force of 40 pounds was applied at t = 14 seconds for a period of 1 second. The initial velocity was 40 feet per second and all other state variables were zero. Figures 18 and 19 clearly show strong similarities, yet there are significant differences apparent. There were at least three reasons for the differences. A much smaller computing increment was used in the program being verified. There was a basic difference in the method of determining braking forces. There was a difference in the method of accounting for "weight shift"

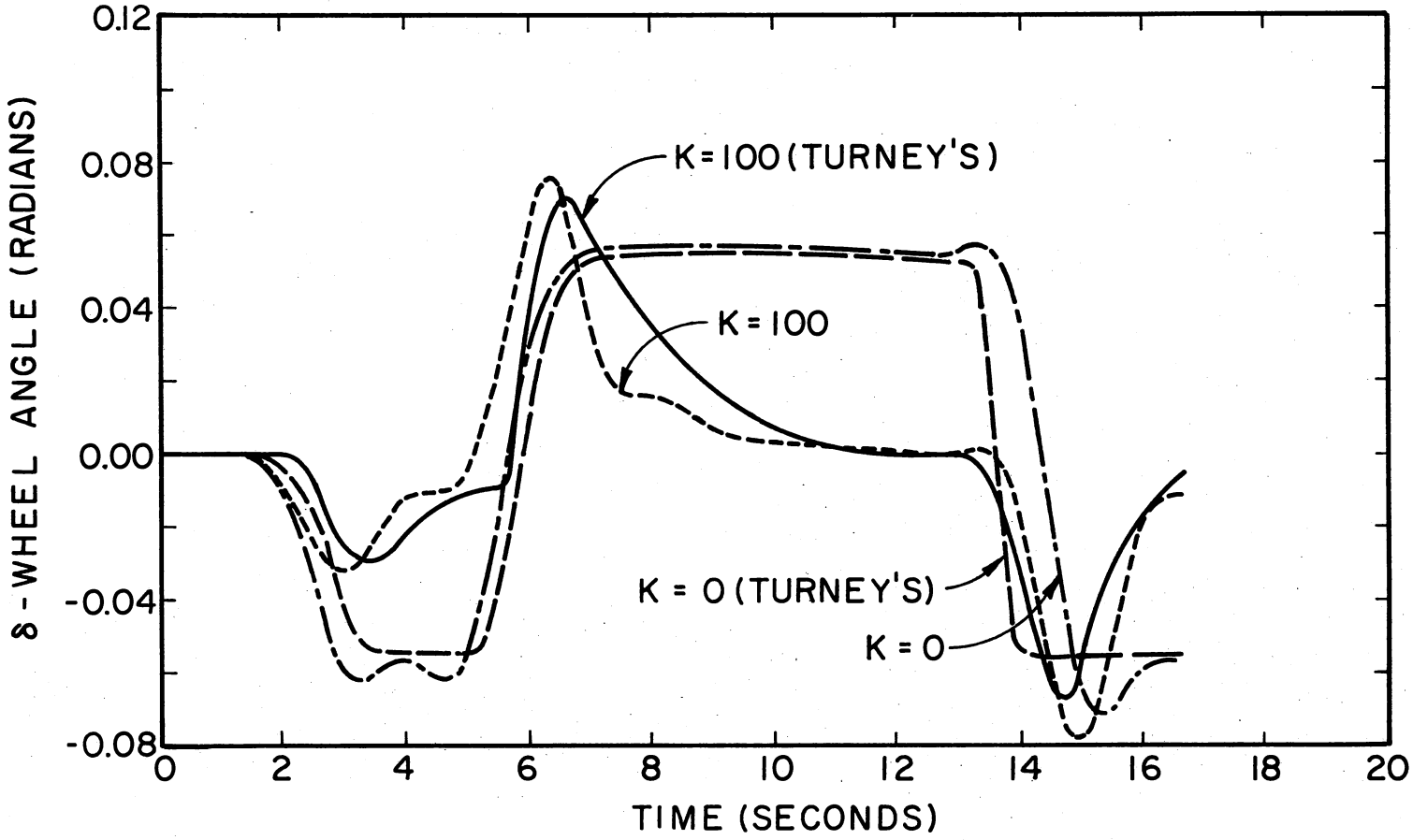

Figure 18. Comparison of Numerical Solutions for Impulse Steering (Front Wheel Steering Angle)(Truck Data--Set 1)

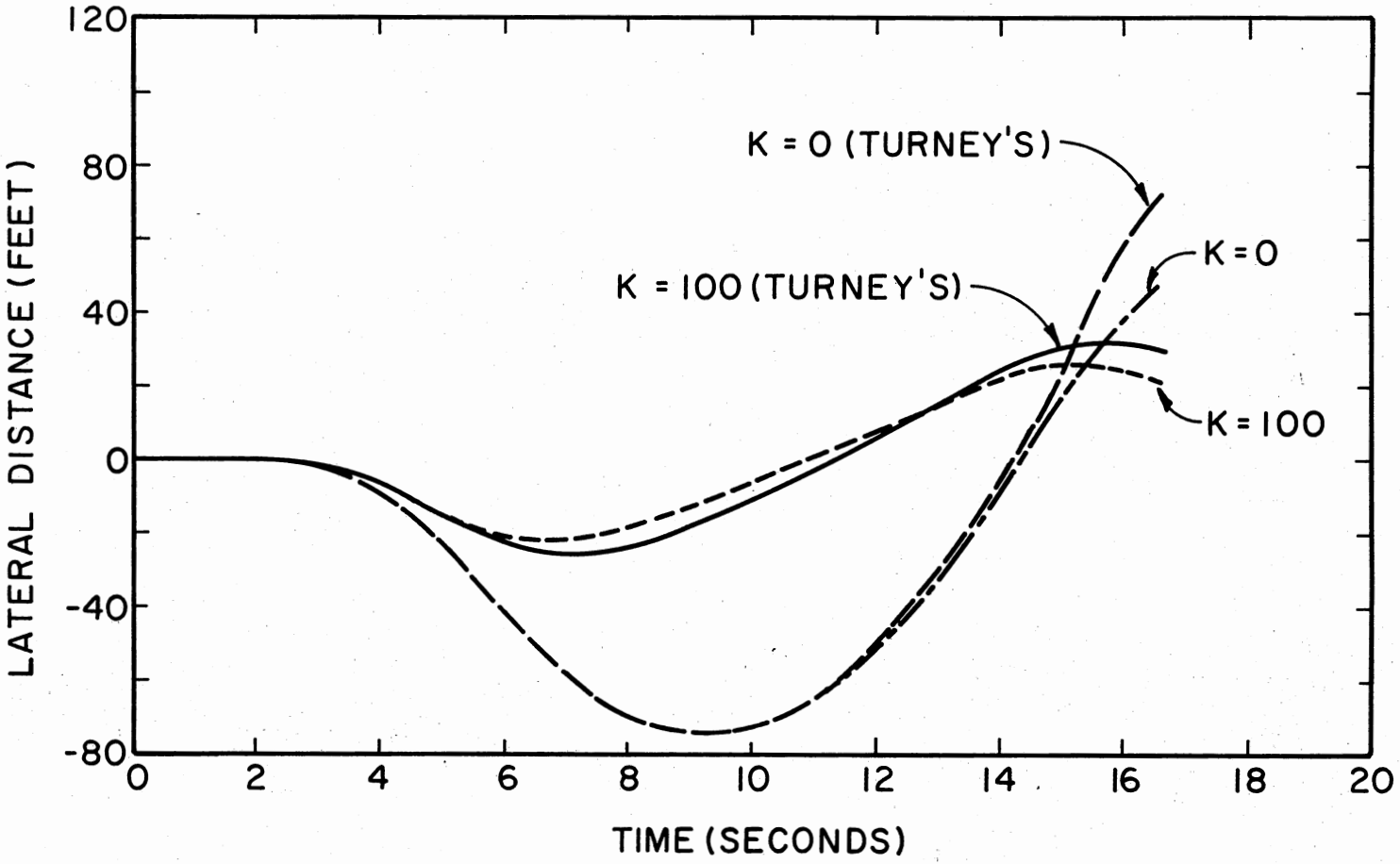

Figure 19. Comparison of Numerical Solutions for Impulse Steering (Lateral Motion of Cab C.G.)(Truck Data--Set 1)

due to forward inertia. The results were quite similar, however, and did not merit further investigation for the purposes of this research.

The third case of comparison also utilized results obtained from the study of Reference (1). This case looked at the response of the four degrees-of-freedom system to a blowout of the left front tire. The truck data used were that of set 1 in Table II. The force simulation for the blowout is shown in Figure 20. The steering response of the reference program was used and was given by

$$FSO = C_1\theta + C_2\delta + C_3 \tag{4.1}$$

where $C_1 = 300$, $C_2 = 600$, $C_3 = -26$. The initial velocity was 40 feet per second and all other state variables were zero. The tire was allowed to blowout at t = 2 seconds. The driver did not respond for $1\frac{1}{8}$ seconds. The lateral distance traveled is shown as a function of time in Figure 21 for both the results of this study and those of Reference (1). Just as before, the results of both programs were quite similar but did have minor differences. The differences in results were very likely caused by the same three items mentioned in comparison case two; that is, computing increment, braking force, and weight shift were different in precisely the same manner for this case as for comparison case two. It was concluded that the differences in results for this case were sufficiently small to warrant acceptance of the program as correct unless the results obtained later were physically unreasonable.

Case four was the first comparison case having the trailer attached during a maneuver. The computing increment was .01 seconds. The initial velocity was 40 feet per second with all other state variables zero. The impulse steering forces of comparison case two were used. The truck data were that of set 2 in Table II. Figure 22 shows the steering wheel

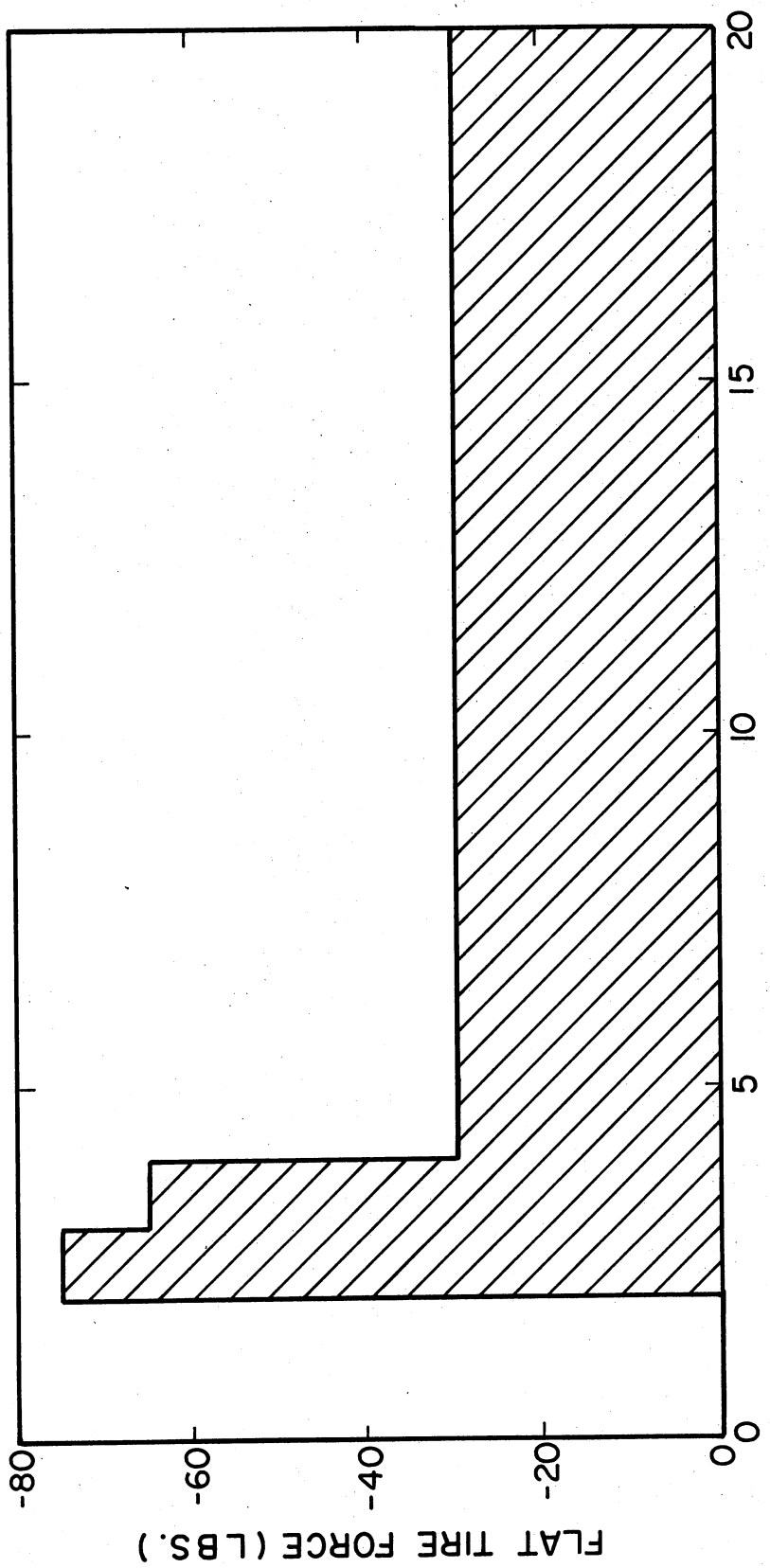

Figure 20. Force Simulation for a Blowout

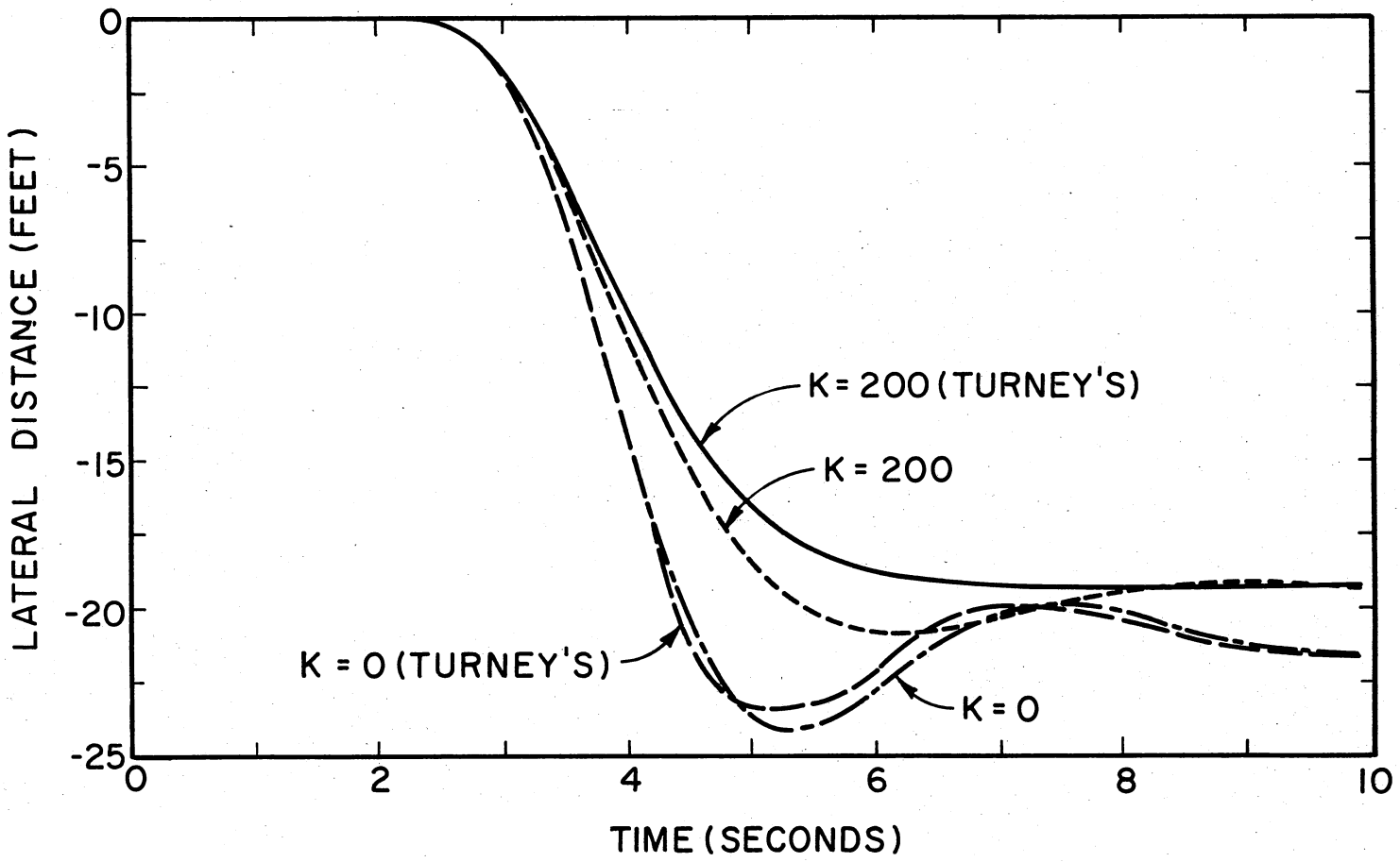

Figure 21. Comparison of Numerical Solutions for Blowout of Left Front Tire (Lateral Motion of Cab C.G.--Truck Data Set 1)

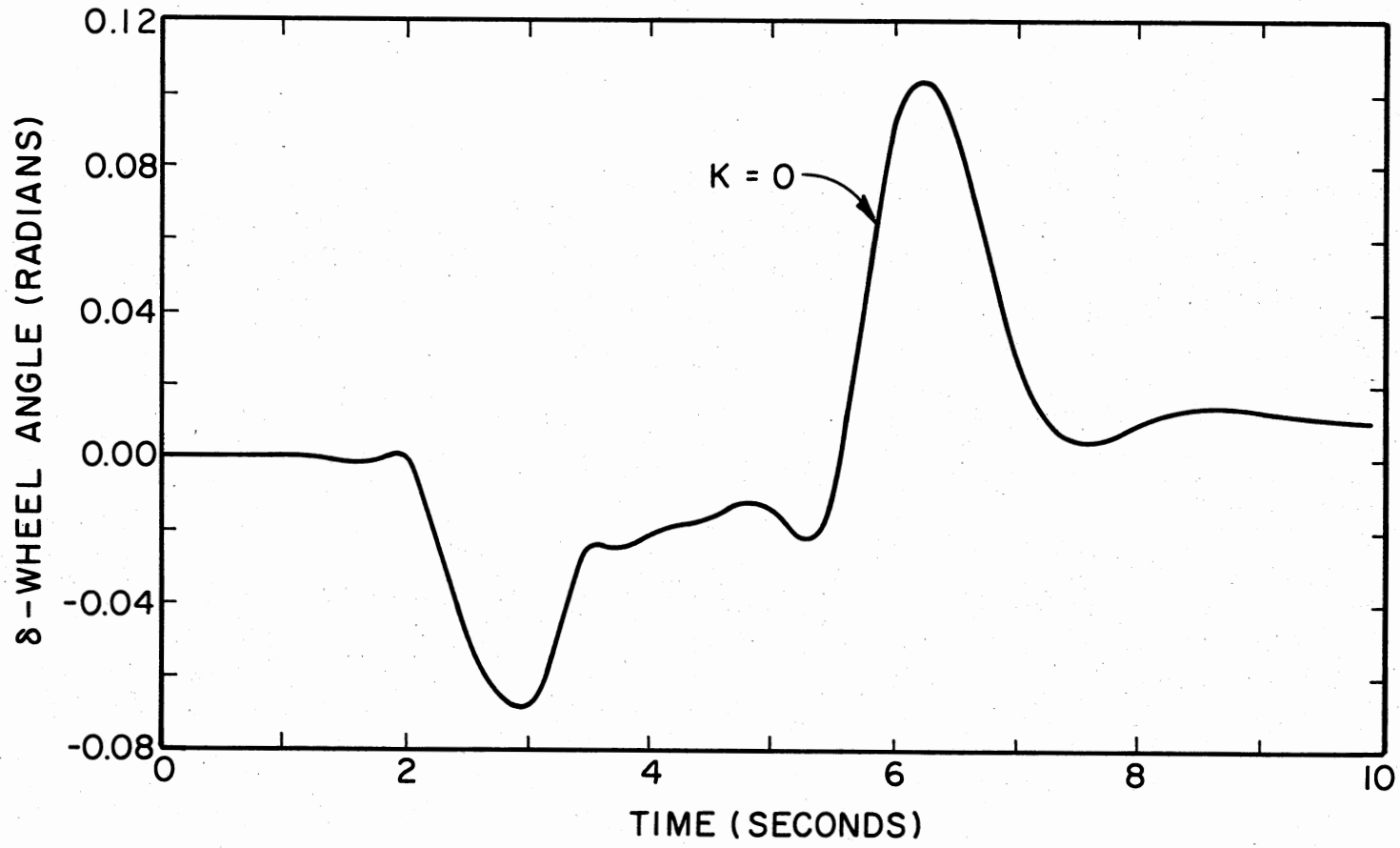

Figure 22. Steering Angle Response to Impulse Steering Force (Truck Data--Set 2)

angle as a function of time. Figure 23 shows the lateral distance traveled as a function of time. Since different wheel characteristics were used for this case than for case two, no quantitative comparisons could be made. There was, however, one very interesting qualitative difference in the two cases. Without the trailer, case two, the front wheel steering angle remained nearly unchanged when the steering force was removed. When the trailer was attached, as in case four, the front wheel steering angle came back toward zero when the steering force was removed. This could not be due to the inherent self-aligning torque characteristics of the front wheels because the program of this study did not include camber or tire deflection. It could only be due to the fact that the trailer had a tendency to steer the tractor slightly during a turning maneuver. This would seem to indicate that a trailer has a centering effect on the front wheels. This particular characteristic may well have been the reason for the interesting result to be discussed later concerning blowouts. Figure 23 simply showed that attaching a trailer had the result of reducing lateral motion for a given steering input. The major contribution to verification of the program by this case was that the results were physically acceptable and meaningful.

This phase of the study concluded the validity investigation of the program. The preceding four cases were considered enough to accept the results of further research if trends and implications were the objective and not precise distances or angles.

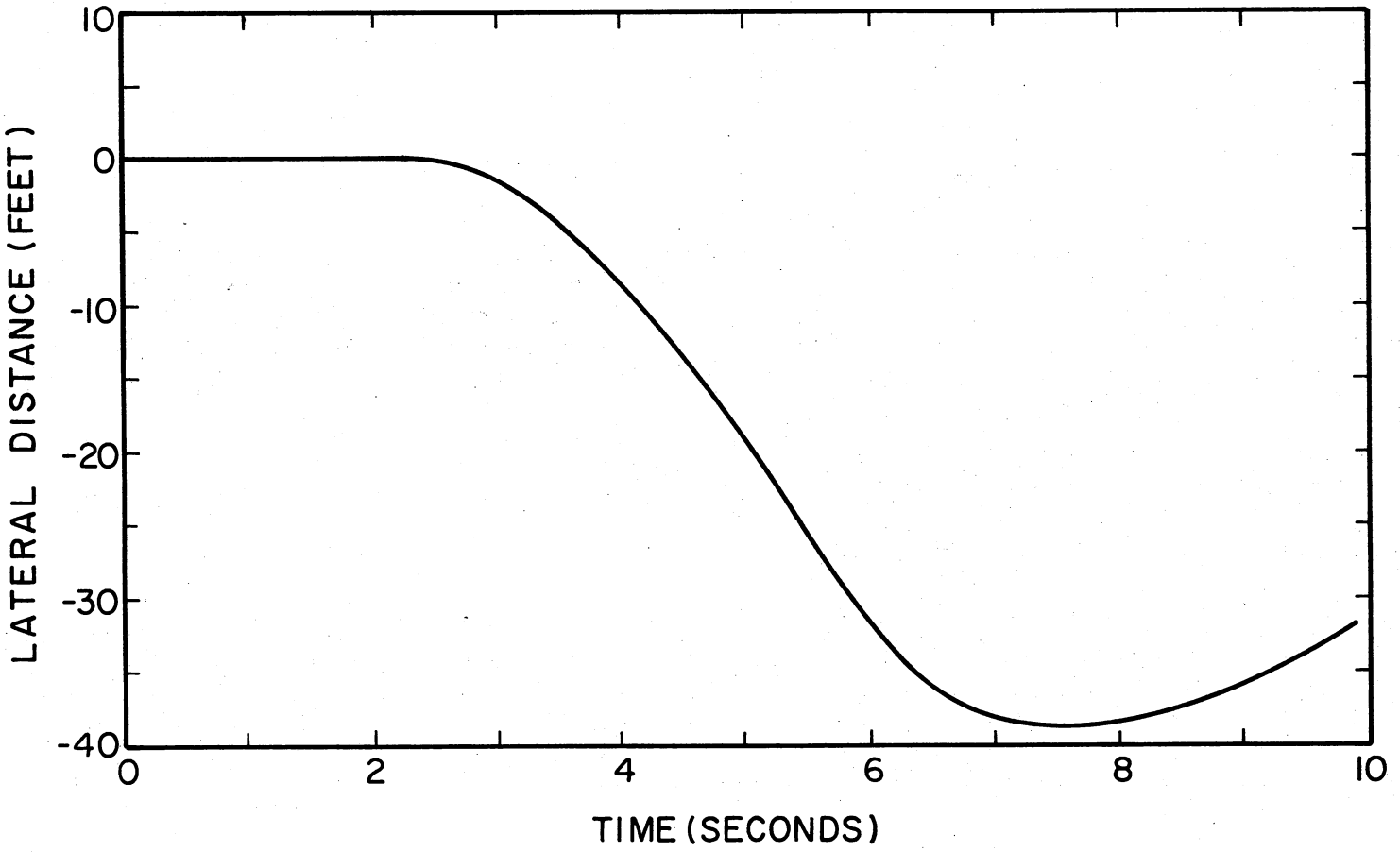

Figure 23. Lateral Translational Response to Impulse Steering Force (Truck Data--Set 2)

Investigation of Stability and Controllability Characteristics of the Articulated Vehicle

After having validated the methodology and the computer program, the trends and implications concerning fifth wheel anti-jackknifing devices and front wheel spring-type centering devices were investigated. There were three cases considered in this section. These cases were selected to allow the investigation of jackknifing, impulse steering, and blowouts with an articulated vehicle.

The first case selected for investigation was that of jackknifing. Because the question of driver response time was the major one of interest, it was necessary to make several assumptions to determine when the driver response should have begun and when the driver would have been incapable of stopping the jackknifing regardless of his response (i.e., when the driver response should have ended). Through physical insight and personal judgment, it was assumed that the driver would recognize a dangerous situation developing when λ reached 2°. For the same reasons mentioned above, it was assumed that the driver would not respond for an additional 1 second due to indecision and reaction time. The above two parameters then determined when driver response should begin. Keller (11) had determined that once λ reached 20°-30° no response by the driver could prevent jackknifing; therefore, driver response was assumed to end once λ reached 25°. It was apparent that these parameters would not produce quantitatively exact results for every person and every vehicle, but because these parameters were used within a comparison situation, the results were correct for qualitative purposes. The truck data used were that of set 2 in Table II. The

initial velocity was 88 feet per second. The initial β and δ angles were .03 radians to simulate a slight turn. All remaining state variables were zero. A computing increment of .01 seconds was used. The steering function was chosen to simulate the driver holding the steering wheel in its initial position. This was done by algebraically manipulating the $\ddot{\beta}$ equation of motion and substituting in the proper values for δ and $\ddot{\delta}$. The brakes were applied on the tractor only and at 2/3 of their maximum unlocked value for wet asphalt because this produced the fastest jackknifing rate. With all the above parameters, it was determined that there were 1.9 seconds response time. In other words, the driver had 1.9 seconds in which to release the brakes and to steer the front wheels in the most advantageous manner.

The above situation used no jackknife prevention device. There were several on the market that could have been attached to the fifth wheel, or even replaced it (such as the "Mather Jackknife Control Unit (10)); therefore, three different types of anti-jackknifing devices were considered for the above mentioned parameters.

The first of the three devices we considered was the "Mather Jackknife Control Unit." It was designed as a damping device and could supply a maximum of 5000 foot-pounds moment. Assuming that this occurred when $\dot{\lambda}$ reached a magnitude of .5 radians per second and that the moment was described by the equation,

$$M\phi MO = C_2\dot{\lambda} \tag{4.2}$$

where C_2 = 10,000. The driver was allowed an additional 1.1 seconds of response time. This was actually a total of 3.0 seconds response time (i.e., a 58% increase over the response time with no anti-jackknifing device).

The second of the three devices was a simple torsional spring device. It was anticipated that comparisons with the "Mather Jackknife Control Unit" would be meaningful; therefore, a spring constant was selected through an iteration process that allowed the driver the same amount of response time (i.e., 3.0 seconds). The equation for the moment was given by

$$M\phi MO = C_1\lambda \tag{4.3}$$

where C_1 = 6100. All other conditions were the same as before.

The third device incorporated the first two and was a function of vehicle speed down the road as well. As mentioned before, it was anticipated that comparisons would be meaningful; therefore, the device was developed to give the same driver response time of 3.0 seconds. The equation describing the moment was given by

$$M\phi MO = (C_3\lambda + C_4\dot{\lambda})\,\dot{R}_x \tag{4.4}$$

where C_3 = 47.2, C_4 = 77.4. All other conditions were the same as before.

It was apparent from these cases that a fifth wheel anti-jackknifing device could significantly increase the driver response time. This, of course, might provide the driver with enough additional time to stop the generation of a high speed jackknife. Figure 24 shows the angle λ as a function of time for (1)--no fifth wheel device, (2)--a spring-type fifth wheel device, (3)--a damper-type fifth wheel device, and (4)--a combination-type fifth wheel device.

The second case selected for investigation was the loss of maneuverability due to the devices used to increase the driver response time. For this set of runs the initial velocity down the road was 25 feet per

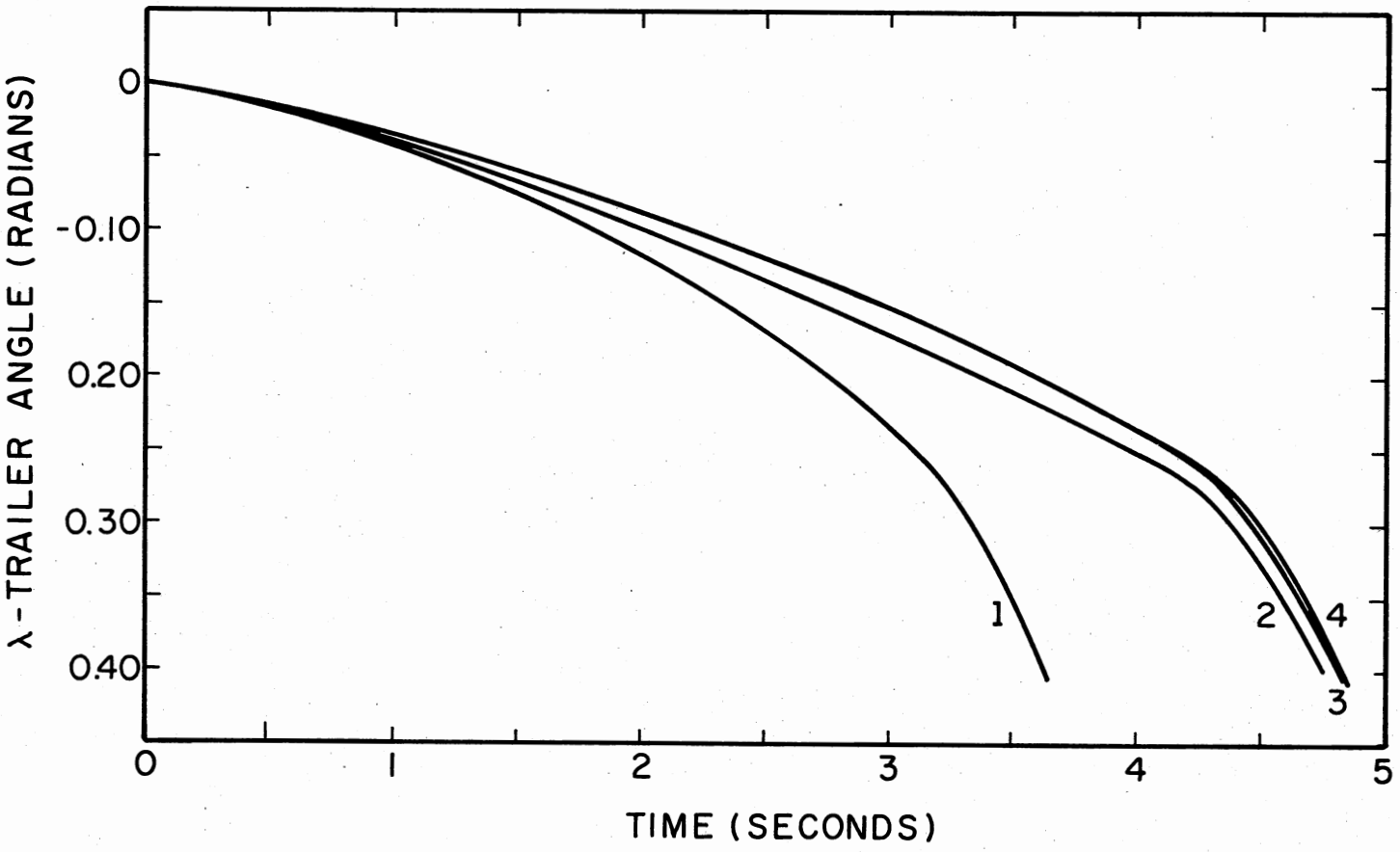

Figure 24. Lambda (Angle Between Tractor and Trailer) Response to Braking Axles 1 and 2 Only (Truck Data--Set 2)

second. All other state variables were initially zero. The truck data were that of set 2 in Table II. The computing increment was .005 seconds. No brakes were applied by the driver but a steering force of 50 pounds was applied at t = 0 seconds. The steering force was removed at t = 1 second. Another steering force of -50 pounds was applied at t = 2 seconds and held through the remainder of the four-second limit on the case. The above series of steering forces were intended to simulate the driver having to respond rapidly in an emergency situation while traveling at a slow speed. Figure 25 shows the lateral distance traveled as a function of time. The numbers identify the particular graph belonging to each fifth wheel device of investigation case one.

It was apparent from Figure 25 that the loss of maneuverability was certainly minimal for the velocity chosen. It was also apparent from Equation (4.3) that the spring device could cause major problems for a driver maneuvering in a parking area. Although the damper device of Equation (4.2) would not hamper parking maneuvers, it did give the poorest showing in Figure 25 by restricting the vehicle to the smallest lateral displacement during an emergency situation. However, the combination device results were most like those of no device at all in the emergency situation described and surely would give no opposition at extreme low speeds while providing all the anti-jackknifing resistance required for relatively safe vehicle operation at high speeds.

The third and final case under investigation focused on the spring-type front wheel centering device. As in comparison case three, a blow-out of the left front tire occurred at t = 2 seconds. The initial velocity was 88 feet per second and all other state variables were zero. The computing increment was .01 seconds. The truck data were that of

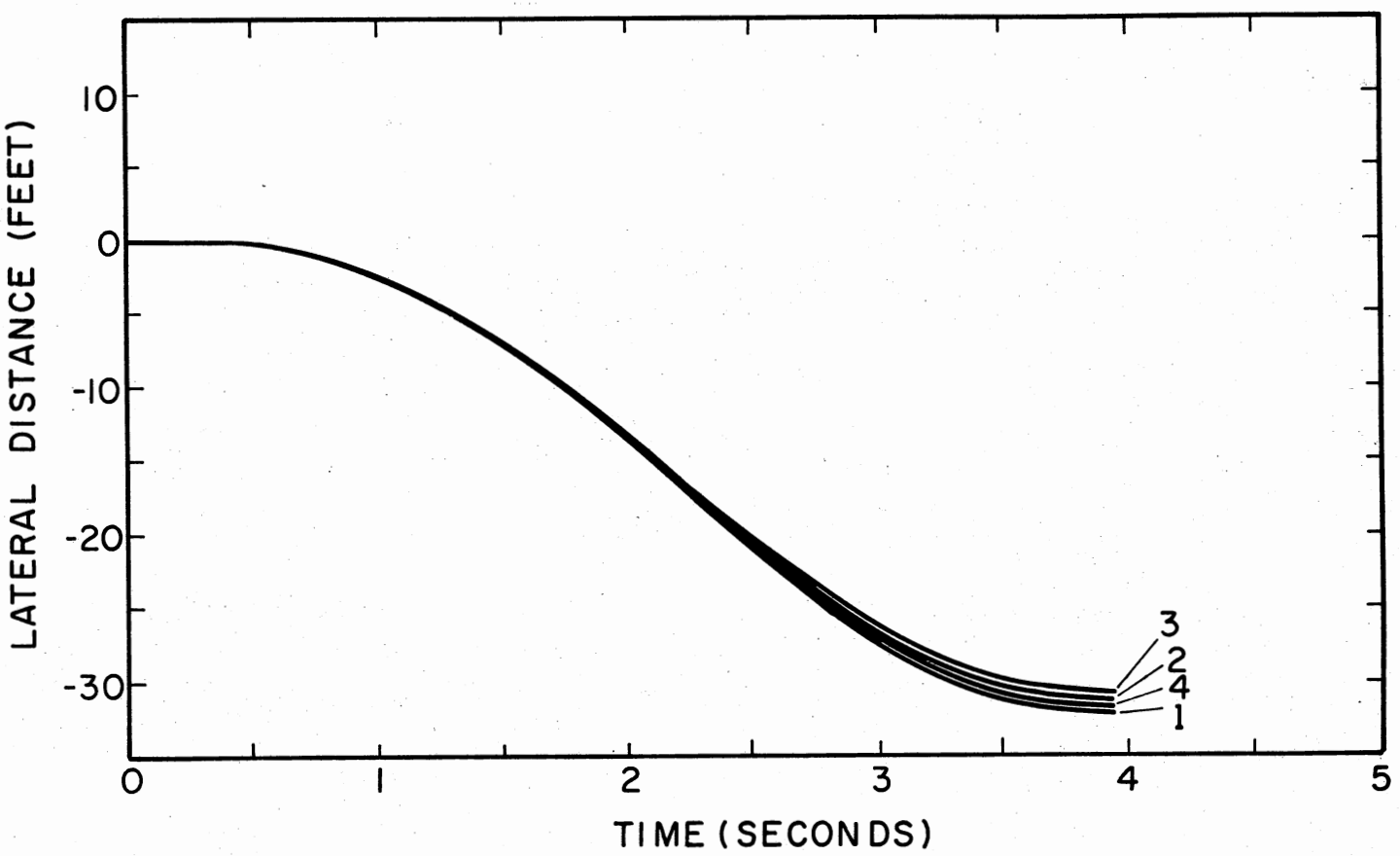

Figure 25. Lateral Translational Response to Impulse Steering Force (Truck Data--Set 2)

set 2 in Table II. The driver was assumed to have the same 1 second delay time described in investigation case one. The steering function was arrived at by analyzing the steady state condition first and then estimating the constants to properly emphasize the state variables a driver is aware of. The function was given by

$$FSO = C_1\theta + C_2\dot{\theta} + C_3\delta + C_4\dot{\delta} + C_5 \tag{4.5}$$

where $C_1 = 300$, $C_2 = 75$, $C_3 = 600$, $C_4 = 150$, and $C_5 = .535/\cos\delta$. The steering function cannot be precisely correct for all situations, but the relative merits of all conditions considered were qualitatively correct because the steering function was the same for each condition. Data were collected for spring constants of zero and 200 on the front wheel centering device with all four possible fifth wheel conditions. Because the data were so nearly identical for the four possible fifth wheel conditions, only the condition of no fifth wheel anti-jackknifing device was documented for this case.

Figure 26 shows the lateral distance traveled as a function of time for both spring constants. It was very interesting to compare the qualitative results of this graph with those of Figure 19. The results in Figure 26 showed that an articulated vehicle with the trailer heavily loaded would travel farther off the road if a spring centering device were used on the front wheels than if no device were used. This was a very significant point. It may perhaps be explained by looking at Figure 27 and by remembering from comparison case four that a trailer had a centering effect on the front wheels. In Figure 27 the front wheel steering angle is shown as a function of time for both spring constants. In the case of no spring device, by the time the driver started to react, the front wheels had already started returning to the neutral

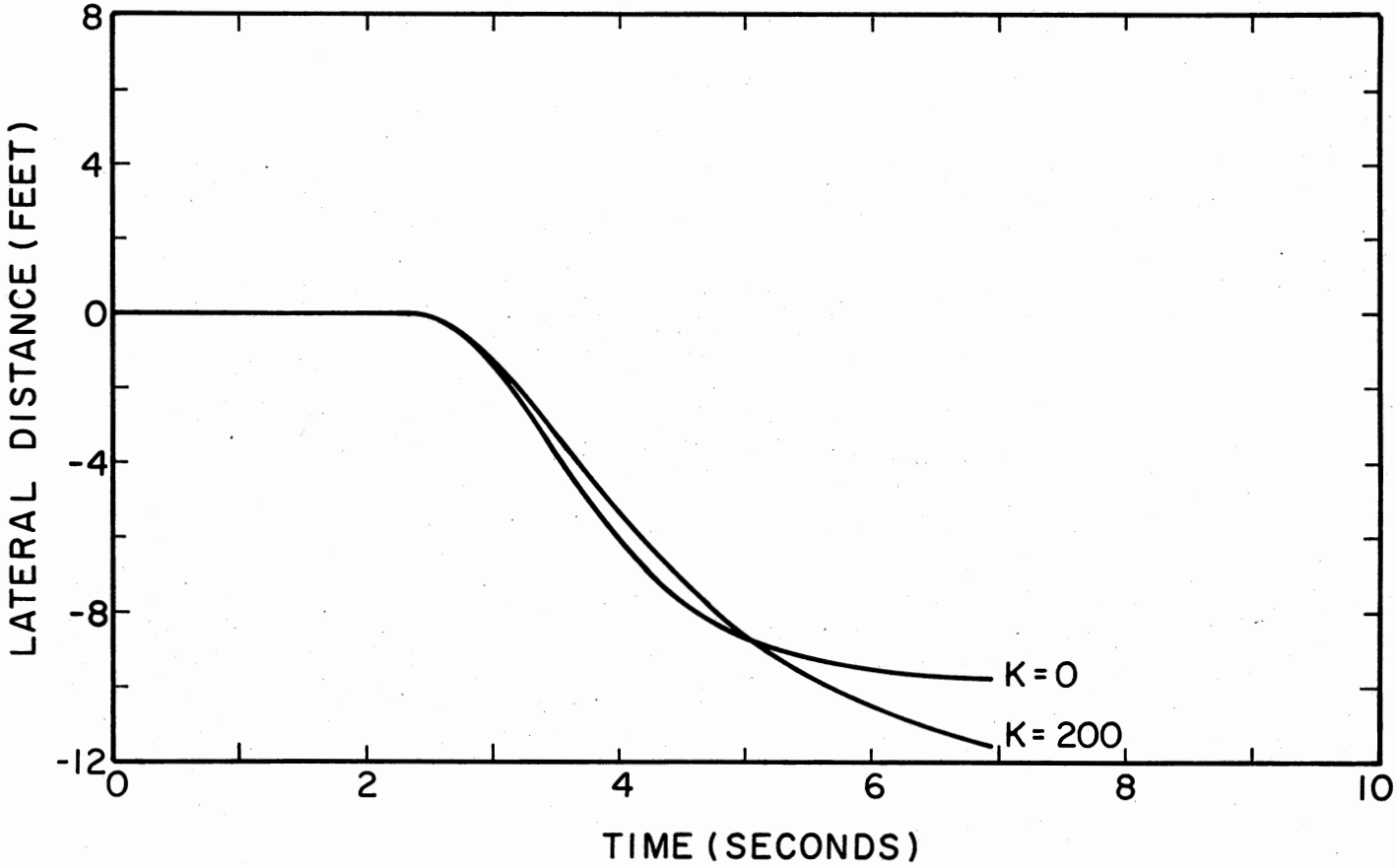

Figure 26. Lateral Translational Response to Left Front Tire Blowout
(F.W. Moment ⇒ None; Truck Data--Set 2)

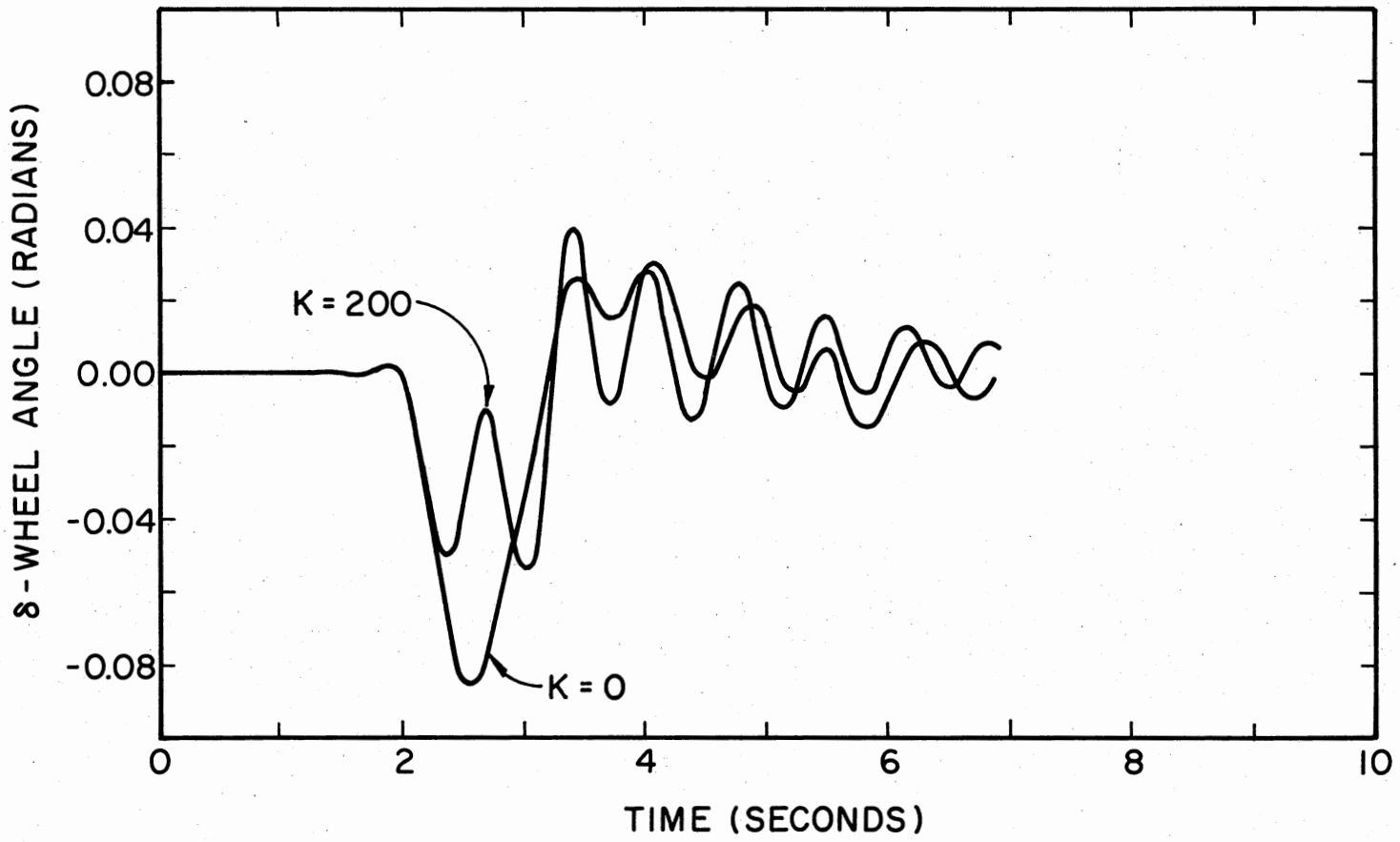

Figure 27. Steering Angle Response to Left Front Tire Blowout
(F.W. Moment ⇒ None; Truck Data--Set 2)

position. In the case of the spring device of K = 200, the front wheels had already returned to the neutral position and started to oscillate away again. In this case, by the time the driver started to respond, he had to overcome the momentum of the steering system and then correct the steering angle. This was a strong indication that a front wheel spring centering device may hinder to some extent a driver's attempt to regain control of his vehicle in a blowout situation.

A valid criticism of spring centering devices should also include an evaluation of the data presented by Figure 28. This figure shows the trailer angle λ plotted as a function of time. Jackknifing would become a serious threat if this angle became too large for a given speed. The spring centering device on the front wheels reduced the maximum angle λ somewhat over that of no device. A more elaborate analysis might show that the effect of a reduced λ would significantly reduce the likelihood of jackknifing.

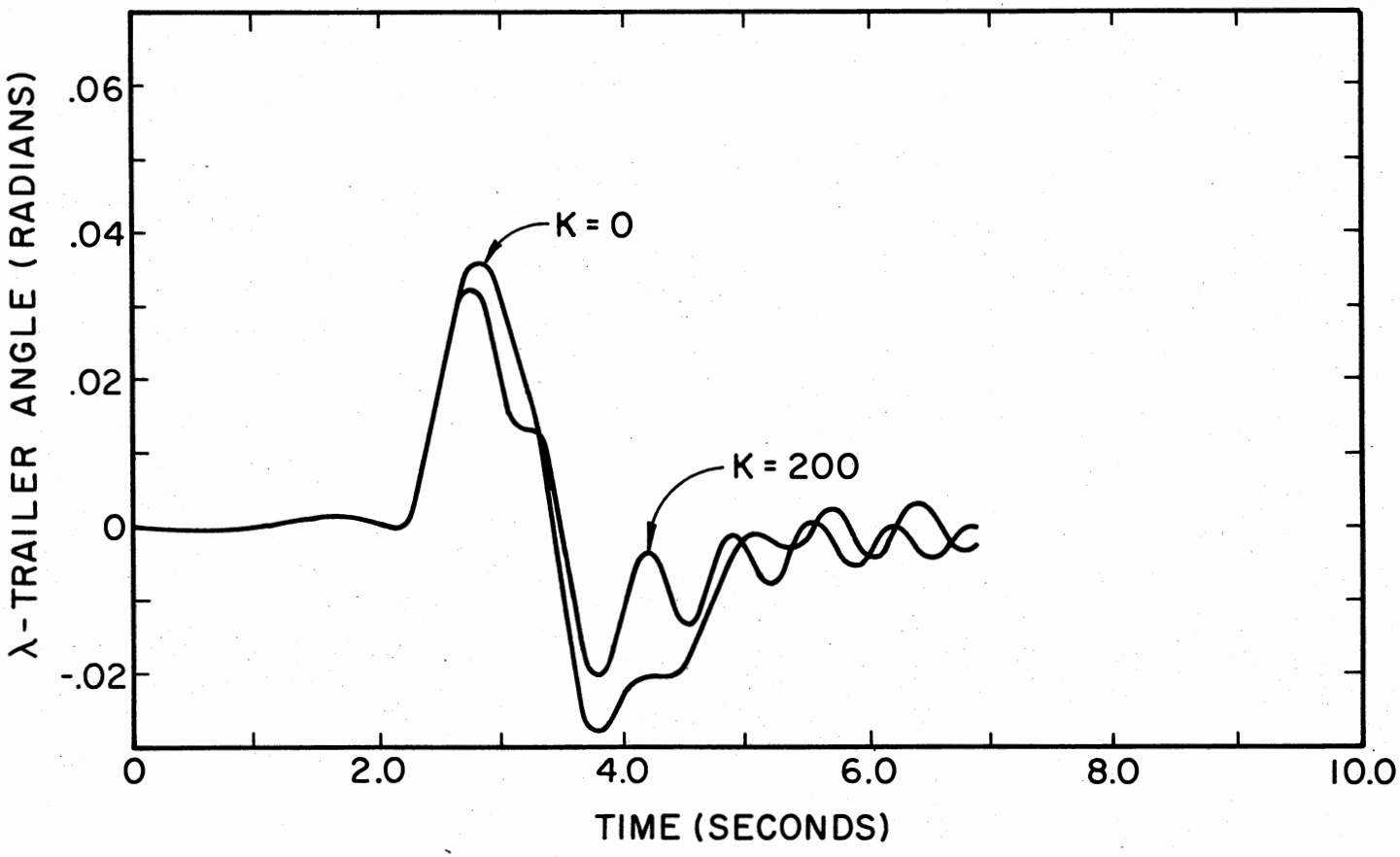

Figure 28. Lambda (Angle Between Tractor and Trailer) Response to Left Front Tire Blowout (F.W. Moment ⇒ None; Truck Data--Set 2)

CHAPTER V

SUMMARY, CONCLUSIONS AND RECOMMENDATIONS

This document reports on an investigation of a typical tractor-semitrailer combination. Because jackknifing presents a severe problem of safety, it was desirable to determine what effect a fifth wheel anti-jackknifing device would have on controlability and jackknifing. It was also desirable to determine what effect a spring-centered steering stabilizer device would have on controlability and jackknifing.

To find the answers to the above problems a five degree-of-freedom model was established. The equations of motion then were derived. To solve the equations of motion a large computer program was developed, verified, and applied. In the collection of data to answer the above problems, three different fifth wheel devices were studied. They were a spring device, a damper device, and a combination device, incorporating both spring and damper characteristics as well as being dependent upon velocity down the road.

The following conclusions have been drawn from this study:

1. A fifth wheel device presently on the market and the hypothetical ones investigated will definitely increase the amount of response time a driver would have in a jackknifing situation (if they are properly designed), thereby decreasing the likelihood of jackknifing going beyond the point of control.

2. Fifth wheel devices may be designed to give the required amount of response time (unless too much time is required) and still not create any loss of desired maneuverability or controllability at slow or high speeds.

3. A spring centered stabilizer device may hinder the natural response of the steering system during a blowout of a front tire on an articulated vehicle. This may cause the vehicle to proceed further beyond the path of control of that vehicle with no device. It will, however, decrease the maximum angle between tractor and trailer and may therefore prevent jackknifing during extreme situations. Fifth wheel devices have an insignificant effect in this case of a blowout.

Recommendations for further study concerning this research are as follows:

1. The results of this study should be compared for verification purposes to results obtained experimentally from an articulated vehicle that closely resembles the simulated model. After the above comparison, the simulated model should be modified to include normal spring suspension and again checked against the results documented in this thesis and against those obtained experimentally.

2. The spring centered steering stabilizer of this study should be investigated further to determine if a change in the spring constant would effect a change in the results of investigation case three. A more elaborate study of the effects of this case should also include attempts to change the natural frequency of the steering system and thereby change the results obtained.

3. The assumptions and techniques used within this study were sufficient to give correct results within the order of magnitude of the

investigation. For a higher order of magnitude investigation, the assumptions and techniques used may not be acceptable; therefore, close inspection should be given to the method of evaluation of tire forces, friction coefficient values, driver steering functions, lack of spring suspension, assumptions made concerning the steering system, and anything else that is viewed to be subject to criticism.

BIBLIOGRAPHY

(1) Turney, D. L. "A Preliminary Study of the Effects of Front Wheel Steering Stabilizers on Vehicle Response Characteristics." (M. S. thesis, Oklahoma State University, 1975.)

(2) Jindra, F. "Tractor and Semi-Trailer Handling." Automobile Engineer, Vol. 53 (1963), pp. 438-446.

(3) Jindra, F. "Handling Characteristics of Tractor-Trailer Combinations." SAE Transactions, Vol. 75 (1965), Paper 650720.

(4) Ellis, J. R. "The Ride and Handling of Semi-Trailer Articulated Vehicles." Automobile Engineer, Vol. 56 (1966), pp. 523-529.

(5) Mikulcik, E. C. "The Dynamics of Tractor-Semitrailer Vehicles: The Jackknifing Problem." SAE Transactions, Vol. 80 (1971), Paper 710045.

(6) Krauter, A. I. and R. K. Wilson. "Simulation of Tractor-Semitrailer Handling." SAE Transactions, Vol. 81 (1972), Paper 720922.

(7) Vincent, R. J. and A. I. Krauter. "Tractor-Semitrailer Handling: A Dynamic Tractor Suspension Model." SAE Transactions, Vol. 82 (1973), Paper 730653.

(8) Leucht, P. M. "The Directional Dynamics of the Commercial Tractor-Semitrailer Vehicle During Braking." SAE Transactions, Vol. 79 (1970), Paper 700371.

(9) Marples, V. "Safety in Trucking Operations." (Report No. ME/A 75-1, Carleton University, 1975.)

(10) Ordorica, M. A. "The Mather Jackknife Control Unit." SAE Transactions, Vol. 82 (1973), Paper 730641.

(11) Keller, A. J. "Jackknife Control for Tractor-Trailer." SAE Transactions, Vol. 82 (1973), Paper 730643.

(12) Walsh, R. C. and G. E. Cicchetti. "Use of Simplified Jackknife Restraint Device Significantly Reduces the Hazard of Jackknifing." SAE Transactions, Vol. 82 (1973), Paper 730642.

(13) Olsson, G. R. "Effects of Tire Slip on the Handling Performance of Tractor-Semitrailers in Braking Maneuvers." SAE Transactions, Vol. 82 (1973), Paper 730184.

(14) Gerald, C. F. Applied Numerical Analysis, 2nd ed. California: Addison-Wesley, 1973.

APPENDIX A

DERIVATION OF $\ddot{\bar{R}}_{p_1}$ and $\ddot{\bar{R}}_{p_2}$

The left front wheel's center of gravity (p_1) displacement with respect to the inertial reference is given by:

$$\bar{R}_{p_1} = \bar{R}_o + \bar{\rho}_1 + \bar{\rho}_2 \tag{A.1}$$

The first derivative with respect to time is:

$$d/dt(\bar{R}_{p_1})_{XYZ} = d/dt[\bar{R}_o + \bar{\rho}_1 + \bar{\rho}_2]_{XYZ} \tag{A.2}$$

which becomes

$$(\dot{\bar{R}}_{p_1})_{XYZ} = \dot{\bar{R}}_o + [(\dot{\bar{\rho}}_1)_{xyz} + (\bar{\omega}_1 \times \bar{\rho}_1)] + [d/dt(\bar{\rho}_2)_{xyz} + (\bar{\omega}_1 \times \bar{\rho}_2)] \tag{A.3}$$

where $\bar{\omega}_1 = \dot{\theta}k$, and further development yields:

$$(\dot{\bar{R}}_{p_1})_{XYZ} = \dot{\bar{R}}_o + (\dot{\bar{\rho}}_1)_{xyz} + (\bar{\omega}_1 \times \bar{\rho}_1) + (\dot{\bar{\rho}}_2)_{x_1y_1z_1} + (\bar{\omega}_3 \times \bar{\rho}_2) \tag{A.4}$$

where $\bar{\omega}_3 = (\dot{\theta} + \dot{\delta})\bar{k} = \dot{\beta}\bar{k}$.

The second derivative with respect to time becomes:

$$\begin{aligned}(\ddot{\bar{R}}_{p_1})_{XYZ} = {} & \ddot{\bar{R}}_o + (\ddot{\bar{\rho}}_1)_{xyz} + (\bar{\omega}_1 \times \dot{\bar{\rho}}_1) \\ & + (\bar{\omega}_1 \times \dot{\bar{\rho}}_1) + (\dot{\bar{\omega}}_1 \times \bar{\rho}_1) + [\bar{\omega}_1 \times (\bar{\omega}_1 \times \bar{\rho}_1)] \\ & + (\ddot{\bar{\rho}}_2)_{x_1y_1z_1} + (\bar{\omega}_3 \times \dot{\bar{\rho}}_2) + (\bar{\omega}_3 \times \dot{\bar{\rho}}_2) \\ & + (\dot{\bar{\omega}}_3 \times \bar{\rho}_2) + [\bar{\omega}_3 \times (\bar{\omega}_3 \times \bar{\rho}_2)]\end{aligned} \tag{A.5}$$

Because of rigid body assumptions:

$$(\ddot{\bar{\rho}}_1)_{xyz} = (\dot{\bar{\rho}}_1)_{xyz} = (\ddot{\bar{\rho}}_2)_{x_1y_1z_1} = (\dot{\bar{\rho}}_2)_{x_1y_1z_1} = 0 \tag{A.6}$$

which reduces Equation (A.5) to:

$$(\ddot{\bar{R}}_{p_1})_{XYZ} = \ddot{\bar{R}}_o + (\dot{\bar{\omega}}_1 \times \bar{\rho}_1) + (\bar{\omega}_1 \times (\bar{\omega}_1 \times \bar{\rho}_1)) + (\dot{\bar{\omega}}_3 \times \bar{\rho}_2) + (\bar{\omega}_3 \times (\bar{\omega}_3 \times \bar{\rho}_2)) \tag{A.7}$$

Similarly for the right front wheel:

$$(\ddot{\bar{R}}_{p_2})_{XYZ} = \ddot{\bar{R}}_o + (\dot{\bar{\omega}}_1 \times \bar{\rho}_3) + (\bar{\omega}_1 \times (\bar{\omega}_1 \times \bar{\rho}_3)) + (\dot{\bar{\omega}}_3 \times \bar{\rho}_4) + (\bar{\omega}_3 \times (\bar{\omega}_3 \times \bar{\rho}_4)) \tag{A.8}$$

Recognizing that,

$$\bar{\rho}_1 = (a\cos\theta + d/2\sin\theta)\bar{i} + (a\sin\theta - d/2\cos\theta)\bar{j} \tag{A.9}$$

$$\bar{\rho}_2 = (e\sin\beta)\bar{i} + (-e\cos\beta)\bar{j} \tag{A.10}$$

and that,

$$\bar{k} \times \bar{i} = \bar{j} \tag{A.11}$$

$$\bar{k} \times \bar{j} = -\bar{i} \tag{A.12}$$

Equation (A.7) can be expressed in specific terms by substituting Equations (A.9, A.10, A.11, A.12) in as:

$$\begin{aligned}\ddot{\bar{R}}_{p_1} = \ddot{\bar{R}}_o &+ [\ddot{\theta}d/2 - \dot{\theta}^2a + \ddot{\beta}e\cos\delta - \dot{\beta}^2e\sin\delta]\bar{i}\cos\theta \\ &+[\ddot{\theta}d/2 - \dot{\theta}^2a + \ddot{\beta}e\cos\delta - \dot{\beta}^2e\sin\delta]\bar{j}\sin\theta \\ &-[\ddot{\theta}a + \dot{\theta}^2d/2 + \ddot{\beta}e\sin\delta + \dot{\beta}^2e\cos\delta]\bar{i}\sin\theta \\ &+[\ddot{\theta}a + \dot{\theta}^2d/2 + \ddot{\beta}e\sin\delta + \dot{\beta}^2e\cos\delta]\bar{j}\cos\theta\end{aligned} \tag{A.13}$$

Recognizing that,

$$\bar{\rho}_3 = (a\cos\theta - d/2\sin\theta)\bar{i} + (a\sin\theta + d/2\cos\theta)\bar{j} \tag{A.14}$$

$$\bar{\rho}_4 = (-e\sin\beta)\bar{i} + (e\cos\beta)\bar{j} \tag{A.15}$$

Equation (A.8) can be expressed in specific terms by substituting in Equations (A.11, A.12, A. 14, A.15) as:

$$\ddot{\bar{R}}_{p_2} = \ddot{\bar{R}}_o$$
$$+ [-\ddot{\theta}d/2 - \dot{\theta}^2 a - \ddot{\beta}e\cos\delta + \dot{\beta}^2 e\sin\delta]\bar{i}\cos\theta$$
$$+ [-\ddot{\theta}d/2 - \dot{\theta}^2 a - \ddot{\beta}e\cos\delta + \dot{\beta}^2 e\sin\delta]\bar{j}\sin\theta$$
$$- [\ddot{\theta}a - \dot{\theta}^2 d/2 - \ddot{\beta}e\sin\delta - \dot{\beta}^2 e\cos\delta]\bar{i}\sin\theta$$
$$+ [\ddot{\theta}a - \dot{\theta}^2 d/2 - \ddot{\beta}e\sin\delta - \dot{\beta}^2 e\cos\delta]\bar{j}\cos\theta \qquad \text{(A.16)}$$

Equations (A.13) and (A.16) are the terms for acceleration for the left front wheel and right front wheel, respectively, with respect to the inertial reference.

APPENDIX B

DERIVATION OF $\ddot{\bar{R}}_{p_3}$

The trailer's center of gravity (p_3) displacement with respect to the inertial reference is given by:

$$\bar{R}_{p_3} = \bar{R}_o + \bar{\rho}_5 + \bar{\rho}_6 \tag{B.1}$$

The first derivative with respect to time is:

$$d/dt[\bar{R}_{p_3}]_{XYZ} = d/dt[\bar{R}_o + \bar{\rho}_5 + \bar{\rho}_6]_{XYZ} \tag{B.2}$$

which becomes:

$$\begin{aligned}(\dot{\bar{R}}_{p_3})_{XYZ} = \dot{\bar{R}}_o &+ [(\dot{\bar{\rho}}_5)_{xyz} + (\bar{\omega}_1 \times \bar{\rho}_5)] \\ &+ [d/dt(\bar{\rho}_6)_{xyz} + (\bar{\omega}_1 + \bar{\rho}_6)]\end{aligned} \tag{B.3}$$

and with further development:

$$\begin{aligned}(\dot{\bar{R}}_{p_3})_{XYZ} = \dot{\bar{R}}_o &+ (\dot{\bar{\rho}}_5)_{xyz} + (\bar{\omega}_1 \times \bar{\rho}_5) \\ &+ (\dot{\bar{\rho}}_6)_{x_3y_3z_3} + (\bar{\omega}_5 \times \bar{\rho}_6)\end{aligned} \tag{B.4}$$

where $\bar{\omega}_5 = (\dot{\theta} + \dot{\lambda})\bar{k} = \dot{\sigma}\bar{k}$.

The second derivative with respect to time becomes:

$$\begin{aligned}(\ddot{\bar{R}}_{p_3})_{XYZ} = \ddot{\bar{R}}_o &+ (\ddot{\bar{\rho}}_5)_{xyz} + (\bar{\omega}_1 \times \dot{\bar{\rho}}_5) \\ &+ (\bar{\omega}_1 \times \dot{\bar{\rho}}_5) + (\dot{\bar{\omega}}_1 \times \bar{\rho}_5) + (\bar{\omega}_1 \times (\bar{\omega}_1 \times \bar{\rho}_5)) \\ &+ (\ddot{\bar{\rho}}_6)_{x_3y_3z_3} + (\bar{\omega}_5 \times \dot{\bar{\rho}}_6) \\ &+ (\bar{\omega}_5 \times \dot{\bar{\rho}}_6) + (\dot{\bar{\omega}}_5 \times \bar{\rho}_6) + (\bar{\omega}_5 \times (\bar{\omega}_5 \times \bar{\rho}_6))\end{aligned} \tag{B.5}$$

Because of rigid body assumptions,

$$(\ddot{\bar{\rho}}_5)_{xyz} = (\dot{\bar{\rho}}_5)_{xyz} = (\ddot{\bar{\rho}}_6)_{x_3y_3z_3} = (\dot{\bar{\rho}}_6)_{x_3y_3z_3} = 0 \qquad (B.6)$$

which reduces Equation (B.5) to:

$$(\ddot{\bar{R}}_{p_3})_{XYZ} = \ddot{\bar{R}}_o + (\dot{\bar{\omega}}_1 \times \bar{\rho}_5) + (\bar{\omega}_1 \times (\bar{\omega}_1 \times \bar{\rho}_5)) + (\dot{\bar{\omega}}_5 \times \bar{\rho}_6) + (\bar{\omega}_5 \times (\bar{\omega}_5 \times \bar{\rho}_6)) \qquad (B.7)$$

Recognizing that

$$\bar{\rho}_5 = (-b\cos\theta)\bar{i} + (-b\sin\theta)\bar{j} \qquad (B.8)$$

$$\bar{\rho}_6 = (-\ell\cos\sigma)\bar{i} + (-\ell\sin\sigma)\bar{j} \qquad (B.9)$$

Equation (B.7) can be expressed in specific terms by substituting Equations (A.11, A.12, B.8, B.9) in as:

$$\begin{aligned}(\ddot{\bar{R}}_{p_3})_{XYZ} = \ddot{\bar{R}}_o &+ [\dot{\theta}^2 b + \ddot{\sigma}\ell\sin\lambda + \dot{\sigma}^2\ell\cos\lambda]\bar{i}\cos\theta \\ &+ [\dot{\theta}^2 b + \ddot{\sigma}\ell\sin\lambda + \dot{\sigma}^2\ell\cos\lambda]\bar{j}\sin\theta \\ &- [-\ddot{\theta}b - \ddot{\sigma}\ell\cos\lambda + \dot{\sigma}^2\ell\sin\lambda]\bar{i}\sin\theta \\ &+ [-\ddot{\theta}b - \ddot{\sigma}\ell\cos\lambda + \dot{\sigma}^2\ell\sin\lambda]\bar{j}\cos\theta \qquad (B.10)\end{aligned}$$

Equation (B.10) is the term for acceleration of the trailer center of gravity with respect to the inertial reference.

APPENDIX C

DERIVATION OF $\ddot{\beta}$

Newton's Equations of Motion for the free-body diagram of Figure 4 are:

$$m_{w1}a_{p_1y} = R_{y1} + F_{s1} + F_{y1}\cos\delta + F_{x1}\sin\delta \tag{C.1}$$

$$m_{w1}a_{p_1x} = R_{x1} - F_{y1}\sin\delta + F_{x1}\cos\delta \tag{C.2}$$

$$I_{w1}\ddot{\beta}_1 = -k\delta - F_{s1}(s\cos\delta + e\sin\delta) - R_{y1}e\sin\delta - R_{x1}e\cos\delta \tag{C.3}$$

where a_{p_1y} is the y-axis projection of $\ddot{\bar{R}}_{p_1}$ and a_{p_1x} is the x-axis projection of $\ddot{\bar{R}}_{p_1}$ and are given by:

$$a_{p_1y} = -\ddot{R}_X\sin\theta + \ddot{R}_Y\cos\theta + a\ddot{\theta} + d/2\dot{\theta}^2 + e\ddot{\beta}\sin\delta + e\dot{\beta}^2\cos\delta \tag{C.4}$$

$$a_{p_1x} = \ddot{R}_X\cos\theta + \ddot{R}_Y\sin\theta + d/2\ddot{\theta} - a\dot{\theta}^2 + e\ddot{\beta}\cos\delta - e\dot{\beta}^2\sin\delta \tag{C.5}$$

Solving Equations (C.1) and (C.2) for R_{y1} and R_{x1}, respectively, yields:

$$R_{y1} = m_{w1}a_{p_1y} - F_{s1} - F_{y1}\cos\delta - F_{x1}\sin\delta \tag{C.6}$$

$$R_{x1} = m_{w1}a_{p_1x} + F_{y1}\sin\delta - F_{x1}\cos\delta \tag{C.7}$$

Substituting Equations (C.4) and (C.5) into Equations (C.6) and (C.7), then substituting the values obtained into Equation (C.3) and reducing yields:

$$\ddot{\beta}_1 = (I_{w1} + m_{w1}e^2)^{-1}\begin{bmatrix} -k\delta - sF_{s1}\cos\delta + eF_{x1} \\ -m_{w1}e\begin{bmatrix}(-\ddot{R}_X\sin\theta + \ddot{R}_Y\cos\theta)\sin\delta \\ + (\ddot{R}_X\cos\theta + \ddot{R}_Y\sin\theta)\cos\delta \\ (a\sin\delta + d/2\cos\delta)\ddot{\theta} \\ (d/2\sin\delta - a\cos\delta)\dot{\theta}^2\end{bmatrix}\end{bmatrix} \tag{C.8}$$

Newton's Equations of Motion for the free-body diagram of Figure 5 are:

$$m_{w2}a_{p_2y} = R_{y2} + F_{s2} + F_{x2}\sin\delta + F_{y2}\cos\delta \quad (C.9)$$

$$m_{w2}a_{p_2x} = R_{x2} + F_{x2}\cos\delta - F_{y2}\sin\delta \quad (C.10)$$

$$I_{w2}\ddot{\beta}_2 = -k\delta - F_{s2}(s\cos\delta - e\sin\delta) + R_{x2}e\cos\delta + R_{y2}e\sin\delta \quad (C.11)$$

where a_{p_2y} is the y-axis projection of $\ddot{\bar{R}}_{p_2}$ and a_{p_2x} is the x-axis projection of $\ddot{\bar{R}}_{p_2}$ and are given by:

$$a_{p_2y} = -\ddot{R}_X\sin\theta + \ddot{R}_Y\cos\theta + a\ddot{\theta} - d/2\dot{\theta}^2 - e\ddot{\beta}\sin\delta - e\dot{\beta}^2\cos\delta \quad (C.12)$$

$$a_{p_2x} = \ddot{R}_X\cos\theta + \ddot{R}_Y\sin\theta - d/2\ddot{\theta} - a\dot{\theta}^2 - e\ddot{\beta}\cos\delta + e\dot{\beta}^2\sin\delta \quad (C.13)$$

Solving Equations (C.9) and (C.10) for R_{y2} and R_{x2}, respectively, yields:

$$R_{y2} = m_{w2}a_{p_2y} - F_{s2} - F_{x2}\sin\delta - F_{y2}\cos\delta \quad (C.14)$$

$$R_{x2} = m_{w2}a_{p_2x} - F_{x2}\cos\delta + F_{y2}\sin\delta \quad (C.15)$$

Substituting Equations (C.12) and (C.13) into Equations (C.14) and (C.15), then substituting the values obtained into Equations (C.11) and reducing yields:

$$\ddot{\beta}_2 = (I_{w2} + m_{w2}e^2)^{-1}\left[\begin{array}{l} -k\delta - sF_{s2}\cos\delta - eF_{x2} \\ +m_{w2}e\left[\begin{array}{l}(\ddot{R}_X\cos\theta + \ddot{R}_Y\sin\theta)\cos\delta \\ +(-\ddot{R}_X\sin\theta + \ddot{R}_Y\cos\theta)\sin\delta \\ +(a\sin\delta - d/2\cos\delta)\ddot{\theta} \\ +(-a\cos\delta - d/2\sin\delta)\dot{\theta}^2\end{array}\right]\end{array}\right] \quad C.16)$$

It is required that $m_{w1} = m_{w2}$, $I_{w1} = I_{w2}$, and $\ddot{\beta}_1 = \ddot{\beta}_2$. Equating Equations (C.8) and (C.16) and reducing yields:

$$(F_{s2} - F_{s1})s\cos\delta = -e(F_{x1} + F_{x2}) + 2m_w e \begin{bmatrix} (-\ddot{R}_X \sin\theta + \ddot{R}_Y \cos\theta)\sin\delta \\ +(\ddot{R}_X \cos\theta + \ddot{R}_Y \sin\theta)\cos\delta \\ +a\ddot{\theta}\sin\delta - a\dot{\theta}^2\cos\delta \end{bmatrix} \qquad (C.17)$$

It is also required that $F_s = F_{s1} + F_{s2}$, combining this with Equation (C.17), substituting into Equation (C.16) and reducing yields:

$$\ddot{\beta} = (I_w + m_w e^2)^{-1} \begin{bmatrix} -k\delta - \frac{1}{2} F_s s\cos\delta + \frac{1}{2} e(F_{x1} - F_{x2}) \\ -m_w ed/2(\ddot{\theta}\cos\delta + \dot{\theta}^2 \sin\delta) \end{bmatrix} \qquad (C.18)$$

This is the complete equation of motion for the front wheel angle with respect to the inertial reference.

APPENDIX D

DERIVATION OF $\ddot{\sigma}$

Newton's Equations of Motion for the free-body diagram of Figure 6:

$$m_T a_{p_3 y} = (F_{y5} + F_{y6})\cos\lambda + (F_{x5} + F_{x6})\sin\lambda - R_{Ty} \tag{D.1}$$

$$m_T a_{p_3 x} = -(F_{y5} + F_{y6})\sin\lambda + (F_{x5} + F_{x6})\cos\lambda - R_{Tx} \tag{D.2}$$

$$I_T\ddot{\sigma} = -M + R_{Tx}\ell\sin\lambda - R_{Ty}\ell\cos\lambda - (F_{y5} + F_{y6})m + (F_{x5} - F_{x6})n/2 \tag{D.3}$$

where $a_{p_3 y}$ is the y-axis projection of $\ddot{\bar{R}}_{p_3}$ and $a_{p_3 x}$ is the x-axis projection of $\ddot{\bar{R}}_{p_3}$ and are given by:

$$a_{p_3 y} = -\ddot{R}_X\sin\theta + \ddot{R}_Y\cos\theta - b\ddot{\theta} - \ell\ddot{\sigma}\cos\lambda + \ell\dot{\sigma}^2\sin\lambda \tag{D.4}$$

$$a_{p_3 x} = \ddot{R}_X\cos\theta + \ddot{R}_Y\sin\theta + b\dot{\theta}^2 + \ell\ddot{\sigma}\sin\lambda + \ell\dot{\sigma}^2\cos\lambda \tag{D.5}$$

Solving Equations (D.1) and (D.2) for R_{Ty} and R_{Tx}, respectively, yields:

$$R_{Ty} = (F_{y5} + F_{y6})\cos\lambda + (F_{x5} + F_{x6})\sin\lambda - m_T a_{p_3 y} \tag{D.6}$$

$$R_{Tx} = -(F_{y5} + F_{y6})\sin\lambda + (F_{x5} + F_{x6})\cos\lambda - m_T a_{p_3 x} \tag{D.7}$$

Substituting Equations (D.4) and (D.5) into Equations (D.6) and (D.7), then substituting the values obtained into Equation (D.3) and reducing yields:

$$\ddot{\sigma} = D_1\left[\begin{array}{l} -M - (F_{y5} + F_{y6})(m+\ell) + (F_{x5} - F_{x6})n/2 \\ -m_T\ell\left[(\ddot{R}_X\cos\theta + \ddot{R}_Y\sin\theta)\sin\lambda - (-\ddot{R}_X\sin\theta\right. \\ \qquad \left.+ \ddot{R}_Y\cos\theta)\cos\lambda + b(\dot{\theta}^2\sin\lambda + \ddot{\theta}\cos\lambda)\right] \end{array}\right] \tag{D.8}$$

This is the complete equation of motion for the trailer angle with respect to the inertial reference.

APPENDIX E

DERIVATION OF $\ddot{R}_X$

Newton's Equation of Motion concerning forces in the X-axis direction is written by observing Figure 7:

$$m_c\ddot{R}_X = [-R_{x1} - R_{x2} + F_{x3} + F_{x4} + R_{Tx}]\cos\theta + [R_{y1} + R_{y2} - F_{y3} - F_{y4} - R_{Ty} + F_s]\sin\theta \qquad (E.1)$$

Recall Equations (C.6) and (C.7), (C.14) and (C.15), and (D.6) and (D.7) and substitute them into Equation (E.1):

$$\begin{aligned} m_c\ddot{R}_X = {} & (F_{x3} + F_{x4})\cos\theta - (F_{y3} + F_{y4})\sin\theta + F_s\sin\theta \\ & - (m_w a_{p_1 x} + F_{y1}\sin\delta - F_{x1}\cos\delta)\cos\theta \\ & - (m_w a_{p_2 x} - F_{x2}\cos\delta + F_{y2}\sin\delta)\cos\theta \\ & + (-m_T a_{p_3 x} - (F_{y5} + F_{y6})\sin\lambda + (F_{x5} + F_{x6})\cos\lambda)\cos\theta \\ & + (m_w a_{p_1 y} - F_{s1} - F_{y1}\cos\delta - F_{x1}\sin\delta)\sin\theta \\ & + (m_w a_{p_2 y} - F_{s2} - F_{x2}\sin\delta - F_{y2}\cos\delta)\sin\theta \\ & - (-m_T a_{p_3 y} + (F_{y5} + F_{y6})\cos\lambda + (F_{x5} + F_{x6})\sin\lambda)\sin\theta \end{aligned} \qquad (E.2)$$

Recall Equations (C.4) and (C.5), (C.12) and (C.13), and (D.4) and (D.5) and substitute them into Equation (E.2) and reduce:

$$\ddot{R}_X = D_2 \begin{bmatrix} (F_{x1} + F_{x2})\cos\delta + (F_{x3} + F_{x4}) + (F_{x5} + F_{x6})\cos\lambda \\ -(F_{y1} + F_{y2})\sin\delta \qquad\qquad - (F_{y5} + F_{y6})\sin\lambda \\ + 2m_w a\dot{\theta}^2 - m_T(b\dot{\theta}^2 + \ell\ddot{\sigma}\sin\lambda + \ell\dot{\sigma}^2\cos\lambda) \end{bmatrix}$$

$$+ D_3 \begin{bmatrix} -(F_{x1} + F_{x2})\sin\delta \qquad\qquad -(F_{x5} + F_{x6})\sin\lambda \\ -(F_{y1} + F_{y2})\cos\delta - (F_{y3} + F_{y4}) - (F_{y5} + F_{y6})\cos\lambda \\ +2m_w a\ddot{\theta} + m_T(-b\ddot{\theta} - \ell\ddot{\sigma}\cos\lambda + \ell\dot{\sigma}^2\sin\lambda) \end{bmatrix} \qquad \text{(E.3)}$$

where $D_2 = \cos\theta/(m_c + 2m_w + m_T)$ and $D_3 = \sin\theta/(m_c + 2m_w + m_T)$. This is the complete equation of motion for the R_X degree-of-freedom.

APPENDIX F

DERIVATION OF $\ddot{R}_Y$

Newton's Equation of Motion concerning forces in the Y-axis direction is written by observing Figure 7, as,

$$m_c\ddot{R}_Y = [-R_{x1} - R_{x2} + F_{x3} + F_{x4} + R_{Tx}]\sin\theta + [-R_{y1} - R_{y2} + F_{y3} + F_{y4} + R_{Ty} - F_s]\cos\theta \qquad (F.1)$$

Recall Equations (C.6) and (C.7), (C.14) and (C.15), and (D.6) and (D.7) and substitute them into Equation (F.1) and reduce:

$$\begin{aligned} m_c\ddot{R}_Y = {} & (F_{x3} + F_{x4})\sin\theta + (F_{y3} + F_{y4})\sin\theta - F_s\cos\theta \\ & - (m_w a_{p_1 x} + F_{y1}\sin\delta - F_{x1}\cos\delta)\sin\theta \\ & - (m_w a_{p_2 x} - F_{x2}\cos\delta + F_{y2}\sin\delta)\sin\theta \\ & + (-m_T a_{p_3 x} - (F_{y5} + F_{y6})\sin\lambda + (F_{x5} + F_{x6})\cos\lambda)\sin\theta \\ & - (m_w a_{p_1 y} - F_{s1} - F_{y1}\cos\delta - F_{x1}\sin\delta)\cos\theta \\ & - (m_w a_{p_2 y} - F_{s2} - F_{x2}\sin\delta - F_{y2}\cos\delta)\cos\theta \\ & + (-m_T a_{p_3 y} + (F_{y5} + F_{y6})\cos\lambda + (F_{x5} + F_{x6})\sin\lambda)\cos\theta \end{aligned} \qquad (F.2)$$

Recall Equations (C.4) and (C.5), (C.12) and (C.13), and (D.4) and (D.5) and substitute them into Equation (F.2) and reduce:

$$\ddot{R}_Y = D_2 \begin{bmatrix} (F_{x1} + F_{x2})\sin\delta & & + (F_{x5} + F_{x6})\sin\lambda \\ + (F_{y1} + F_{y2})\cos\delta + (F_{y3} + F_{y4}) + (F_{y5} + F_{y6})\cos\lambda \\ -2m_w a\ddot{\theta} - m_T(-b\ddot{\theta} - \ell\ddot{\sigma}\cos\lambda + \ell\dot{\sigma}^2\sin\lambda) \end{bmatrix}$$

$$+ D_3 \begin{bmatrix} (F_{x1} + F_{x2})\cos\delta + (F_{x3} + F_{x4}) + (F_{x5} + F_{x6})\cos\lambda \\ -(F_{y1} + F_{y2})\sin\delta & & - (F_{y5} + F_{y6})\sin\lambda \\ +2m_w a\dot{\theta}^2 - m_T(b\dot{\theta}^2 + \ell\ddot{\sigma}\sin\lambda + \ell\dot{\sigma}^2\cos\lambda) \end{bmatrix} \qquad \text{(F.3)}$$

where D_2 and D_3 are as defined in Appendix E. This completely describes the R_Y degree-of-freedom.

APPENDIX G

DERIVATION OF $\ddot{\theta}$

Newton's Equation of Motion concerning moments about the Z-axis is written by observing Figure 7 as:

$$I_c\ddot{\theta} = a(-R_{y1} - R_{y2} - F_s) + b(-F_{y3} - F_{y4} - R_{Ty}) + d/2(R_{x2} - R_{x1}) + w/2(F_{x3} - F_{x4}) + M + 2k\delta \qquad (G.1)$$

Recall Equations (C.6) and (C.7), (C.14) and (C.15), and (D.6) and (D.7) and substitute them into Equation (G.1) and reduce:

$$\begin{aligned} I_c\ddot{\theta} = {} & -aF_s - b(F_{y3} + F_{y4}) + w/2(F_{x3} - F_{x4}) + M + 2k\delta \\ & -a\begin{bmatrix} m_w a_{p_1 y} - F_{s1} - F_{y1}\cos\delta - F_{x1}\sin\delta \\ +m_w a_{p_2 y} - F_{s2} - F_{x2}\sin\delta - F_{y2}\cos\delta \end{bmatrix} \\ & -b\left[-m_T a_{p_3 y} + (F_{y5} + F_{y6})\cos\lambda + (F_{x5} + F_{x6})\sin\lambda\right] \\ & +d/2\begin{bmatrix} m_w a_{p_2 x} - F_{x2}\cos\delta + F_{y2}\sin\delta \\ -m_w a_{p_1 x} - F_{y1}\sin\delta + F_{x1}\cos\delta \end{bmatrix} \end{aligned} \qquad (G.2)$$

Recall Equations (C.4) and (C.5), (C.12) and (C.13), and (D.4) and substitute them into (G.2) and reduce:

$$\ddot{\theta} = -aD_4\begin{bmatrix} -(F_{x1} + F_{x2})\sin\delta - (F_{y1} + F_{y2})\cos\delta \\ +m_w(-2\ddot{R}_X\sin\theta + 2\ddot{R}_Y\cos\theta) \end{bmatrix}$$

$$-bD_4 \begin{bmatrix} (F_{x5} + F_{x6})\sin\lambda + (F_{y3} + F_{y4}) + (F_{y5} + F_{y6})\cos\lambda \\ -m_T \begin{bmatrix} -\ddot{R}_X \sin\theta + \ddot{R}_Y \cos\theta \\ -\ell\ddot{\sigma}\cos\lambda + \ell\dot{\sigma}^2 \sin\lambda \end{bmatrix} \end{bmatrix}$$

$$-d/2D_4 \begin{bmatrix} -(F_{x1} - F_{x2})\cos\delta + (F_{y1} - F_{y2})\sin\delta \\ +2m_w(e\ddot{\beta}\cos\delta - e\dot{\beta}^2 \sin\delta) \end{bmatrix}$$

$$+D_4 [M + 2k\delta + w/2(F_{x3} - F_{x4})] \qquad \text{(G.3)}$$

where D_4 is $1/\{I_c + 2m_w(a^2 + [d/2]^2) + m_T b^2\}$. This equation completely describes the θ degree-of-freedom.

APPENDIX H

DERIVATION OF z_1, z_2, and z_3

Figures 9 and 10 are used in the derivation of the axial normal loads. To determine the normal load on the front axle (z_1), the moments are summed about the y-axis through a point in contact with the road and directly beneath the tractor rear axle.

$$0 = z_1(a + b) - 2w_w(a + b) - w_c(b) - R_{Tx}(h_{Fw}) + m_w(a_{p_1x} + a_{p_2x})(h_w) + m_c a_{cx}(h_c) \quad (H.1)$$

Recall Equations (C.5) and (C.13) and (D.5) and (D.7), substitute them into Equation (H.1) and rearrange to obtain:

$$z_1 = 2m_w g + m_c g(bD_5) + (h_{Fw}D_5)\left[-(F_{y5} + F_{y6})\sin\lambda + (F_{x5} + F_{x6})\cos\lambda\right] \left[-m_T\left[\ddot{R}_X\cos\theta + \ddot{R}_Y\sin\theta \right.\right.$$
$$\left.\left. + b\dot{\theta}^2 + \ell\ddot{\sigma}\sin\lambda + \ell\dot{\sigma}^2\cos\lambda\right]\right]$$
$$- (m_w h_w D_5)2[\ddot{R}_X\cos\theta + \ddot{R}_Y\sin\theta - a\dot{\theta}^2]$$
$$- (m_c h_c D_5)[\ddot{R}_X\cos\theta + \ddot{R}_Y\sin\theta] \quad (H.2)$$

where $D_5 = 1/(a + b)$. This completely describes the normal load on the front axle.

To develop the equation of the normal load on the tractor rear axle (z_2), the moments are summed about the y-axis through a point in

contact with the road and directly beneath the front axle.

$$0 = -z_2(a + b) - R_{Tx}(h_{Fw}) + R_{Tz}(a + b) + w_c(a)$$
$$+ m_c a_{cx}(h_c) + m_w h_w(a_{p_1 x} + a_{p_2 x}) \qquad (H.3)$$

Recall Equations (C.5) and (C.13) and (D.5) and (D.7), substitute them into Equation (H.3) and rearrange to obtain:

$$z_2 = m_c g(aD_5)$$
$$- (h_{Fw}D_5)\left[-(F_{y5} + F_{y6})\sin\lambda + (F_{x5} + F_{x6})\cos\lambda\right.$$
$$\left. - m_T\left[\ddot{R}_X\cos\theta + \ddot{R}_Y\sin\theta \right.\right.$$
$$\left.\left. + b\dot{\theta}^2 + \ell\ddot{\sigma}\sin\lambda + \ell\dot{\sigma}^2\cos\lambda\right]\right]$$
$$+ R_{Tz}$$
$$+ (m_c h_c D_5)[\ddot{R}_X\cos\theta + \ddot{R}_Y\sin\theta]$$
$$+ (m_w h_w D_5)2[\ddot{R}_X\cos\theta + \ddot{R}_Y\sin\theta - a\dot{\theta}^2] \qquad (H.4)$$

The variable R_{Tz} in Equation (H.4) must be defined before the normal load on the second axle may be determined.

To determine the internal force R_{Tz} an inspection of Figure 10 is necessary. The moments must be summed about the $(y)_T$-axis through a point directly beneath the trailer axle.

$$0 = R_{Tz}(m + \ell) + (R_{Tx})_T(h_{Fw}) - w_T(m)$$
$$+ m_T(a_{p_3 x}\cos\lambda + a_{p_3 y}\sin\lambda)(h_T) \qquad (H.5)$$

The variables $(R_{Tx})_T$ and $(R_{Ty})_T$ are the fifth wheel forces transformed to act along the trailer axes. They are described as

$$(R_{Tx})_T = R_{Tx}\cos\lambda + R_{Ty}\sin\lambda \qquad (H.6)$$

$$(R_{Ty})_T = -R_{Tx}\sin\lambda + R_{Ty}\cos\lambda \qquad (H.7)$$

Recall Equations (D.4) and (D.5) and substitute with Equation (H.6) into Equation (H.5), rearranging yields:

$$R_{Tz} = m_T g(mD_6) - (h_{Fw}D_6)[R_{Tx}\cos\lambda - R_{Ty}\sin\lambda] - (m_T h_T D_6)\begin{bmatrix}(\ddot{R}_X\cos\theta + \ddot{R}_Y\sin\theta)\cos\lambda \\ + (-\ddot{R}_X\sin\theta + \ddot{R}_Y\cos\theta)\sin\lambda \\ + b\dot{\theta}^2\cos\lambda - b\ddot{\theta}\sin\lambda + \ell\dot{\sigma}^2\end{bmatrix} \quad (H.8)$$

where $D_6 = 1/(m + \ell)$. Further substitution is still needed; therefore, recall Equations (D.4, D.5, D.6, and D.7), substitute into Equation (H.8) and reduce to obtain:

$$R_{Tz} = m_T g(mD_6) - (h_{Fw}D_6)(F_{x5} + F_{x6}) + [m_T(h_{Fw} - h_T)D_6]\begin{bmatrix}(\ddot{R}_X\cos\theta + \ddot{R}_Y\sin\theta)\cos\lambda \\ + (-\ddot{R}_X\sin\theta + \ddot{R}_Y\cos\theta)\sin\lambda \\ + b\dot{\theta}^2\cos\lambda - b\ddot{\theta}\sin\lambda + \ell\dot{\sigma}^2\end{bmatrix} \quad (H.9)$$

Now that the internal reaction R_{Tz} has been completely defined, it may be substituted into Equation (H.4) and after reduction z_2 is given by:

$$z_2 = m_c g(aD_5) + m_T g(mD_6) - (h_{Fw}D_6)(F_{x5} + F_{x6}) - (h_{Fw}D_5)\begin{bmatrix}-(F_{y5} + F_{y6})\sin\lambda + (F_{x5} + F_{x6})\cos\lambda \\ - m_T\begin{bmatrix}\ddot{R}_X\cos\theta + \ddot{R}_Y\sin\theta \\ + b\dot{\theta}^2 + \ell\ddot{\sigma}\sin\lambda + \ell\dot{\sigma}^2\cos\lambda\end{bmatrix}\end{bmatrix}$$

$$+ [m_T(h_{Fw} - h_T)D_6]\begin{bmatrix}(\ddot{R}_X\cos\theta + \ddot{R}_Y\sin\theta)\cos\lambda \\ + (-\ddot{R}_X\sin\theta + \ddot{R}_Y\cos\theta)\sin\lambda \\ + b\dot{\theta}^2\cos\lambda - b\ddot{\theta}\sin\lambda + \ell\dot{\sigma}^2\end{bmatrix}$$

$$+ (m_c h_c D_5)[\ddot{R}_X \cos\theta + \ddot{R}_Y \sin\theta]$$

$$+ (m_w h_w D_5) 2[\ddot{R}_X \cos\theta + \ddot{R}_Y \sin\theta - a\dot{\theta}^2)] \qquad \text{(H.10)}$$

where D_5 and D_6 are as described earlier. This completely describes the normal load on the tractor rear axle.

To determine the normal load on the trailer axle, another inspection of Figure 10 is required. Summing moments about the $(y)_T$-axis through the fifth wheel yields:

$$0 = -z_3(m + \ell) + (F_{x5} + F_{x6})h_{Fw} + m_T g(\ell)$$

$$+ m_T(h_T - h_{Fw})[a_{p_3 x}\cos\lambda + a_{p_3 y}\sin\lambda] \qquad \text{(H.11)}$$

Recall Equations (D.4) and (D.5), substitute Equation (H.11) and rearrange to obtain:

$$z_3 = D_6[(F_{x5} + F_{x6})h_{Fw} + m_T g(\ell)]$$

$$+ [m_T(h_T - h_{Fw})D_6] \begin{bmatrix} (\ddot{R}_X \cos\theta + \ddot{R}_Y \sin\theta)\cos\lambda \\ + (-\ddot{R}_X \sin\theta + \ddot{R}_Y \cos\theta)\sin\lambda \\ + b\dot{\theta}^2 \cos\lambda - b\ddot{\theta}\sin\lambda + \ell\dot{\sigma}^2 \end{bmatrix} \qquad \text{(H.12)}$$

This completes the derivation of the axial normal loads.

APPENDIX I

DERIVATION OF TIRE NORMAL LOADS (F_{zi})

Figures 11, 12 and 13 show free-body diagrams of the front axle, tractor rear axle, and trailer axle. Included in these figures are the forces which determine the amount of total axle load carried by each tire. It is required that

$$F_{z1} + F_{z2} = Z_1 \tag{I.1}$$

$$F_{z3} + F_{z4} = Z_2 \tag{I.2}$$

$$F_{z5} + F_{z6} = Z_3 \tag{I.3}$$

For Figure 11 summing moments about the x-axis through the point A will give

$$0 = -(F_{z1} - F_{z2})(d/2 + e) + m_w(a_{p_1y} + a_{p_2y})h_w + m_{cF}a_{cy}h_c \tag{I.4}$$

It is assumed that

$$m_{cF} = b/(a + b)m_c \tag{I.5}$$

$$m_{cA} = a/(a + b)m_c \tag{I.6}$$

Recall Equations (C.4) and (C.12) along with (I.1) and (I.5) and substitute into Equation (I.4), reducing yields:

$$\begin{aligned} F_{z1} = {} & (m_w h_w D_7)2[-\ddot{R}_X \sin\theta + \ddot{R}_Y \cos\theta + a\ddot{\theta}] \\ & + \frac{1}{2} Z_1 \\ & + (m_c h_c D_7)(bD_5)[-\ddot{R}_X \sin\theta + \ddot{R}_Y \cos\theta] \end{aligned} \tag{I.7}$$

where $D_7 = 1/(d + 2e)$.

Rewriting Equation (I.1) gives:

$$F_{z2} = Z_1 - F_{z1} \tag{I.8}$$

Following the same procedure for the rear axle as for the front, the summation of moments about the x-axis through point B from Figure 12 gives:

$$0 = -(F_{z3} - F_{z4})(w/2) + m_{cA}a_{cy}h_c - R_{Ty}h_{Fw} \tag{I.9}$$

Recall Equations (D.4) and (D.6) along with (I.2) and (I.6) and substitute into Equation (I.9), reducing yields:

$$F_{z3} = (m_c h_c/w)(aD_5)[-\ddot{R}_X\sin\theta + \ddot{R}_Y\cos\theta] + \frac{1}{2}Z_2 - (h_{Fw}/w)\begin{bmatrix}(F_{y5} + F_{y6})\cos\lambda + (F_{x5} + F_{x6})\sin\lambda \\ - m_T\begin{bmatrix}-\ddot{R}_X\sin\theta + \ddot{R}_Y\cos\theta \\ -b\ddot{\theta} - \ell\ddot{\sigma}\cos\lambda + \ell\dot{\sigma}^2\sin\lambda\end{bmatrix}\end{bmatrix} \tag{I.10}$$

Rewriting Equation (I.2) gives:

$$F_{z4} = Z_2 - F_{z3} \tag{I.11}$$

Again following the same procedure as before, the summation of moments about the $(x)_T$-axis through point C from Figure 13 gives:

$$0 = -(F_{z5} - F_{z6})(n/2) + (R_{Ty})_T h_{Fw} + m_T(a_{p_3y})_T h_T \tag{I.12}$$

Recall Equations (H.6, D.4, D.5, D.6, D.7, I.3) and recognize that

$$(a_{p_3y})_T = -a_{p_3x}\sin\lambda + a_{p_3y}\cos\lambda \tag{I.13}$$

and substitute into Equation (I.12), reduction gives:

$$F_{z5} = (h_{Fw}/n)\begin{bmatrix}(F_{y5} + F_{y6}) + m_T\ell\ddot{\sigma} \\ +m_T\sin\lambda(\ddot{R}_X\cos\theta + \ddot{R}_Y\sin\theta + b\dot{\theta}^2) \\ -m_T\cos\lambda(-\ddot{R}_X\sin\theta + \ddot{R}_Y\cos\theta - b\ddot{\theta})\end{bmatrix}$$

$$+ (m_T h_T/n) \begin{bmatrix} -\ell\ddot{\sigma} - \sin\lambda(\ddot{R}_X\cos\theta + \ddot{R}_Y\sin\theta + b\dot{\theta}^2) \\ +\cos\lambda(-\ddot{R}_X\sin\theta + \ddot{R}_Y\cos\theta - b\ddot{\theta}) \end{bmatrix} \qquad (I.14)$$

$$+ \frac{1}{2} Z_3$$

Rewriting Equation (I.3) gives:

$$F_{z6} = Z_3 - F_{z5} \qquad (I.15)$$

Equations (I.7, I.8, I.10, I.12, I.14, I.15) completely describe the normal load on the tires.

APPENDIX J

DERIVATION OF α_F, α_R, and α_T

Recall Equation (A.4) and substitute into it Equations (A.6, A.9, A.10) and $\bar{\omega}_1 = \dot{\theta}\bar{k}$ and $\bar{\omega}_3 = \dot{\beta}\bar{k}$ to obtain:

$$(\dot{\bar{R}}_{p_1})_{XYZ} = [\dot{R}_X + \dot{\theta}(d/2\cos\theta - a\sin\theta) + \dot{\beta}e\cos\beta]\bar{i} + [\dot{R}_Y + \dot{\theta}(a\cos\theta + d/2\sin\theta) + \dot{\beta}e\sin\beta]\bar{j} \qquad (J.1)$$

The wheel heading angle (ε_F) is expressible as:

$$\varepsilon_F = -\frac{1}{2}\pi + \theta + \delta \qquad (J.2)$$

Therefore, the front wheel slip angle (α_F) is:

$$\alpha_F = \varepsilon_F + \tan^{-1}\left[\frac{\dot{R}_X + \dot{\theta}(d/2\cos\theta - a\sin\theta) + \dot{\beta}e\cos\beta}{\dot{R}_Y + \dot{\theta}(a\cos\theta + d/2\sin\theta) + \dot{\beta}e\sin\beta}\right] \qquad (J.3)$$

With q defined as the point of road contact for the rear tractor wheels, then the position vector is:

$$\bar{R}_q = \bar{R}_o + \bar{\rho}_7 \qquad (J.4)$$

where

$$\bar{\rho}_7 = (-b\cos\theta - w/2\sin\theta)\bar{i} + (-b\sin\theta + w/2\cos\theta)\bar{j} \qquad (J.5)$$

then,

$$\dot{\bar{R}}_q = \dot{\bar{R}}_o + (\bar{\omega}_1 \times \bar{\rho}_7) \qquad (J.6)$$

assuming $\dot{\bar{\rho}}_7 = 0$ (i.e., rigid body motion).

Recall Equations (2.1) and (J.5) and substitute into Equation (J.6) to obtain:

$$\dot{\bar{R}}_q = [\dot{R}_X + \dot{\theta}(b\sin\theta - w/2\cos\theta)]\bar{i} + [\dot{R}_Y + \dot{\theta}(-b\cos\theta - w/2\sin\theta)]\bar{j}$$

The wheel heading angle (ε_R) is expressible as:

$$\varepsilon_R = -\frac{1}{2}\pi + \theta \tag{J.7}$$

Therefore, the rear wheel slip angle (α_R) is:

$$\alpha_R = \varepsilon_R + \tan^{-1}\left[\frac{\dot{R}_X + \dot{\theta}(b\sin\theta - w/2\cos\theta)}{\dot{R}_Y + \dot{\theta}(-b\cos\theta - w/2\sin\theta)}\right] \tag{J.8}$$

With j defined as the point of road contact for the trailer wheels, then the position vector is:

$$\bar{R}_j = \bar{R}_o + \bar{\rho}_5 + \bar{\rho}_8 \tag{J.9}$$

where

$$\bar{\rho}_5 = (-b\cos\theta)\bar{i} + (-b\sin\theta)\bar{j} \tag{J.10}$$

$$\bar{\rho}_8 = [-(\ell + m)\cos\sigma - n/2\sin\sigma]\bar{i} + [-(\ell + m)\sin\sigma + n/2\cos\sigma]\bar{j} \tag{J.11}$$

then,

$$\dot{\bar{R}}_j = \dot{\bar{R}}_o + (\bar{\omega}_1 \times \bar{\rho}_5) + (\bar{\omega}_3 \times \bar{\rho}_8) \tag{J.12}$$

assuming rigid body motion. Recall Equation (2.1) and $\bar{\omega}_1 = \dot{\theta}\bar{k}$ and $\bar{\omega}_3 = \dot{\beta}\bar{k}$ and substitute into Equation (J.12) to obtain:

$$\dot{\bar{R}}_j = [\dot{R}_X + \dot{\theta}b\sin\theta + \dot{\sigma}\{(\ell + m)\sin\sigma - n/2\cos\sigma\}]\bar{i} + [\dot{R}_Y - \dot{\theta}b\cos\theta + \dot{\sigma}\{-(\ell + m)\cos\sigma - n/2\sin\sigma\}]\bar{j} \tag{J.13}$$

The wheel heading angle (ε_T) is expressible as:

$$\varepsilon_T = -\frac{1}{2}\pi + \theta + \lambda \tag{J.14}$$

Therefore, the trailer wheel slip angle (α_T) is:

$$\alpha_T = \varepsilon_T + \tan^{-1}\left[\frac{\dot{R}_X + \dot{\theta}b\sin\theta + \dot{\sigma}\{(\ell+m)\sin\sigma - n/2\cos\sigma\}}{\dot{R}_Y - \dot{\theta}b\cos\theta + \dot{\sigma}\{-(\ell+m)\cos\sigma - n/2\sin\sigma\}}\right] \tag{J.15}$$

Equations (J.3), (J.8) and (J.15) completely describe the various wheel slip angles.

VITA

Cline Turner Young II

Candidate for the Degree of

Master of Science

Thesis: A PRELIMINARY STUDY OF THE EFFECTS OF A FRONT WHEEL STEERING STABILIZER AND OF FIFTH WHEEL ANTI-JACKKNIFING DEVICES ON ARTICULATED VEHICLE RESPONSE CHARACTERISTICS

Major Field: Mechanical Engineering

Biographical:

Personal Data: Born August 24, 1950, in Duncan, Oklahoma, the son of Mr. and Mrs. R. K. Young.

Education: Graduated from Midwest City High School in May, 1968; received the Degree of Bachelor of Science in 1973 from the United States Merchant Marine Academy; completed the requirements for the Degree of Master of Science at Oklahoma State University in May, 1976.

Professional Experience: Graduate teaching assistant, Oklahoma State University, 1974-1975.